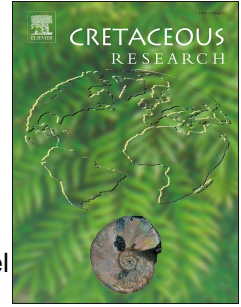


# Journal Pre-proof

A new locality with ctenochasmatid pterosaurs (Pterosauria: Pterodactyloidea) in the Atacama desert, northern Chile

Jhonatan Alarcón-Muñoz, Laura Codorniú, Edwin González, Mario E. Suárez, Manuel Suárez, Omar Vicencio-Campos, Sergio Soto-Acuña, Jonatan Kaluza, Alexander O. Vargas, David Rubilar-Rogers



PII: S0195-6671(22)00037-4

DOI: <https://doi.org/10.1016/j.cretres.2022.105173>

Reference: YCRES 105173

To appear in: *Cretaceous Research*

Received Date: 29 October 2021

Revised Date: 4 February 2022

Accepted Date: 5 February 2022

Please cite this article as: Alarcón-Muñoz, J., Codorniú, L., González, E., Suárez, M.E., Suárez, M., Vicencio-Campos, O., Soto-Acuña, S., Kaluza, J., Vargas, A.O., Rubilar-Rogers, D., A new locality with ctenochasmatid pterosaurs (Pterosauria: Pterodactyloidea) in the Atacama desert, northern Chile, *Cretaceous Research*, <https://doi.org/10.1016/j.cretres.2022.105173>.

This is a PDF file of an article that has undergone enhancements after acceptance, such as the addition of a cover page and metadata, and formatting for readability, but it is not yet the definitive version of record. This version will undergo additional copyediting, typesetting and review before it is published in its final form, but we are providing this version to give early visibility of the article. Please note that, during the production process, errors may be discovered which could affect the content, and all legal disclaimers that apply to the journal pertain.

© 2022 Elsevier Ltd. All rights reserved.

1 **A NEW LOCALITY WITH CTENOCHASMATID PTEROSAURS**  
2 **(PTEROSAURIA: PTERODACTYLOIDEA) IN THE ATACAMA DESERT,**  
3 **NORTHERN CHILE.**

4  
5 Jhonatan Alarcón-Muñoz<sup>a, b</sup>, Laura Codorniú<sup>c</sup>, Edwin González<sup>d</sup>, Mario E. Suárez<sup>e</sup>, Manuel  
6 Suárez<sup>f</sup>, Omar Vicencio-Campos<sup>e</sup>, Sergio Soto-Acuña<sup>a, b</sup>, Jonatan Kaluza<sup>g</sup>, Alexander O.  
7 Vargas<sup>a</sup>, David Rubilar-Rogers<sup>h</sup>

8  
9 <sup>a</sup>Red Paleontológica U-Chile, Laboratorio de Ontogenia y Filogenia, Departamento de  
10 Biología, Facultad de Ciencias, Universidad de Chile, Las Palmeras  
11 3425, Santiago, Chile. [alarconmunoz@ug.uchile.cl](mailto:alarconmunoz@ug.uchile.cl), [sesotacu@ug.uchile.cl](mailto:sesotacu@ug.uchile.cl),  
12 [alexvargas@uchile.cl](mailto:alexvargas@uchile.cl)

13 <sup>b</sup>Kaytreng Consultores. José Domingo Cañas 1640, DP 1502, Ñuñoa, Santiago, Chile.

14 <sup>c</sup>CONICET-Departamento de Geología, Universidad Nacional de San Luis, Avenida  
15 Ejército de Los Andes 950, San Luis 5700, Argentina. [codorniulaura23@gmail.com](mailto:codorniulaura23@gmail.com)

16 <sup>d</sup>Servicio Nacional de Geología y Minería, Avenida Santa María 0104, Providencia,  
17 Santiago, Chile. [edwin.gonzalez@sernageomin.cl](mailto:edwin.gonzalez@sernageomin.cl)

18 <sup>e</sup>Atacama Fósil Research, Avenida Rosario Corvalán 187, Caldera, Atacama, Chile.  
19 [marioesuarz@p@gmail.com](mailto:marioesuarz@p@gmail.com), [omar.vicencio@gmail.com](mailto:omar.vicencio@gmail.com)

20 <sup>f</sup>Universidad Andrés Bello, Carrera de Geología, Avenida República 237, Santiago, Chile.  
21 [manuel.suarez@unab.cl](mailto:manuel.suarez@unab.cl)

22 <sup>g</sup>Fundación de Historia Natural Félix de Azara, Universidad Maimónides, Hidalgo 775,  
23 C1405BCK, CABA, Argentina. [yojonatan@hotmail.com](mailto:yojonatan@hotmail.com)

24 <sup>h</sup>Área de Paleontología, Museo Nacional de Historia Natural, Santiago, Chile, Interior

25 Parque Quinta Normal s/n., Santiago, Chile. [david.rubilar@mnhn.gob.cl](mailto:david.rubilar@mnhn.gob.cl)

26

## 27 **ABSTRACT**

28 We describe a new locality with ctenochasmatid pterosaurs found in a tidal  
29 estuarine paleoenvironment of the Quebrada Monardes Formation (Lower Cretaceous). The  
30 new locality, which is named "Cerro Tormento", is in Cerros Bravos in the northeast  
31 Atacama region, Northern Chile. Here, we describe four cervical vertebrae, one of them  
32 belonging to a small individual, the impression of a right scapulocoracoid, a left coracoid,  
33 an impression of a left humerus, an incomplete left humerus, a distal fragment of the right  
34 humerus, and impressions of a left femur and tibiotarsus. The presence of three humeri and  
35 a cervical vertebra belonging to a small pterosaur indicate that these materials represent  
36 more than one individual. The cervical vertebrae present diagnostic traits shared with  
37 ctenochasmatid pterosaurs, such as elongated vertebral centra, with integrated neural arch,  
38 low neural spines, and dorsally located neural canal. It is currently not possible to  
39 determine if there are one or more species represented. This finding is the second  
40 geographic occurrence of pterosaurs of the clade Ctenochasmatidae in the Atacama region,  
41 and although it is currently uncertain if ctenochasmatids from both locations were  
42 contemporaneous. This suggests that at least one species of the clade Ctenochasmatidae  
43 was widespread in what is now northern Chile. In addition, the presence of bones belonging  
44 to more than one individual preserved in Cerro Tormento suggest that pterosaur colonies  
45 were present at the southwestern margin of Gondwana during the Lower Cretaceous.

46

47 **Keywords:** Pterosauria, Ctenochasmatidae, Quebrada Monardes Formation, Lower  
48 Cretaceous, Chile

49

50 **1. INTRODUCTION**

51           The record of the Pterosauria in Chile is still scarce and most discoveries comprise  
52 fragmentary materials. Until now the most relevant fossil locality that yielded pterosaur  
53 remains in Chile is Cerro La Isla, discovered in 1988 by a team of geologists on the eastern  
54 side east of the Atacama Region (Bell and Suárez, 1989). In that locality previous authors  
55 reported a singular basin with an extensive layer mainly of sandstone and conglomerates  
56 that outcrops on the southern slope of Cerro La Isla, in which apparently hundreds of  
57 disarticulated bones are preserved (Bell and Padian, 1995). These deposits, assigned to  
58 Quebrada Monardes Formation, were interpreted as a result of a sudden flow of sediments  
59 (Bell and Padian, 1995). A rostrum, a possible dentary, and a proximal wing phalanx were  
60 described in 2006 by Martill and collaborators. These authors considered that they  
61 belonged to pterodactyloid pterosaurs of the clade Ctenochasmatidae, a group of pterosaurs  
62 characterized by having long necks and specialized dentition for filter feeding (Martill et  
63 al., 2006). Subsequent work has focused on the study of additional bones collected in that  
64 layer, which suggest that all these bones belong to pterosaurs of the clade  
65 Ctenochasmatidae (Alarcón-Muñoz et al., 2020).

66           In 2013, one of the authors (E.G.) and colleagues fortuitously discovered isolated  
67 bones and bone impressions in loose blocks of sedimentary rocks in Cerros Bravos, in the  
68 northeast Atacama Region. Subsequently, during field work carried out at the locality in  
69 December 2018, the layer in which the bones were preserved was identified (Alarcón-  
70 Muñoz et al., 2018). This locality, called here Cerro Tormento, in reference to the difficulty  
71 to access the site due to the slope and the high altitude (4200 m.a.s.l.), represents a new  
72 occurrence of pterosaurs from the Quebrada Monardes Formation, located approximately

73 65 km north from Cerro La Isla. The field work exposed several bones that were preserved  
74 disarticulated in a layer of sandstones and mud clast breccias, whose characteristics suggest  
75 that they were deposited in a tidal environment, unlike that interpreted in Cerro La Isla.  
76 Here, we describe pterosaur bones from Cerro Tormento. The remains correspond to well-  
77 preserved three-dimensional isolated bones, although mostly incomplete along with bone  
78 impressions. The fact that they are preserved three-dimensionally is particularly important,  
79 since most pterosaur bones are found crushed due to their great fragility (Unwin, 2006).  
80 Among the examples of cretaceous pterosaurs three-dimensionally preserved are important  
81 finds made in Brazil, especially in Lower Cretaceous deposits of the Araripe Basin. Among  
82 these are pterosaurs such as *Tapejara wellnhoferi* Kellner, 1989, and *Caupedactylus ybaka*  
83 Kellner, 2013, among several other findings (e.g. Campos and Kellner, 1985; Kellner et al.,  
84 2013; Cerqueira et al., 2021). Additionally, in Upper Cretaceous rocks of the Goio-Erê  
85 Formation, Manzig et al. (2014) reported the discovery of a bonebed composed of hundreds  
86 of bones of pterosaurs three-dimensionally preserved, most belonging to the tapejarid  
87 *Caiuajara dobruskii* Manzig et al., 2014. A partial specimen preserved at this bonebed was  
88 identified as a different species, which was named *Keresdrakon vilsoni* by Kellner et al.  
89 (2019). The high bone accumulation led Kellner et al. (2019) to name this site as the  
90 "cemitério dos pterossauros".

91 The study of the pterosaur of Cerro Tormento can help answer more accurately  
92 questions related to the phylogenetic affinities of the pterosaurs of the Quebrada Monardes  
93 Formation to other pterosaur species from South America and the rest of the world.

94

## 95 **1.2. Locality and Geological Setting**

96 From the Late Jurassic to the Early Cretaceous, a dominant extensional regime in

97 the southwestern margin of Gondwana, generated several retro-arc basins which were  
98 flooded by marine transgressions. These continental to shallow marine basins were  
99 connected to the proto-Pacific Ocean through narrow passages within the volcanic arc,  
100 characterizing a paleogeography similar to that currently present in the western Pacific  
101 (Chotin, 1981; Mpodozis and Allmendiger, 1993). Some of these marine basins were the  
102 Tarapacá, Chañarcillo and Aconcagua basins (Fig. 1A; Legarreta and Uliana, 1999, Aleman  
103 and Ramos, 2000; Ramos, 2009; Aguirre-Urreta et al., 2007; Ramos et al., 2019)

104 The Chañarcillo Basin was a NNE oriented retro-arc basin, with a linear and narrow  
105 configuration, generated at the east of the Lower Cretaceous volcanic arc (Punta del Cobre  
106 and Aeropuerto Formations) and was filled with volcanic and sedimentary deposits of  
107 shallow marine, paralic and continental depositional environments of the Chañarcillo  
108 Group (Abundancia, Nantoco, Totoralillo and Pabellon formations) and Quebrada  
109 Monardes Formation (Fig. 1B; Mercado, 1982; Arévalo, 1995; Cornejo et al., 1998; Godoy  
110 and Lara, 1998; Lara and Godoy, 1998; Matthews et al., 2006; Mpodozis et al., 2012;  
111 Cornejo et al., 2013; Contreras et al., 2014; Mpodozis et al., 2018).

112 This stratigraphic record represents the last of the back-arc marine episodes in the  
113 north of Chile and gives evidence of the existence of corridors along which marine currents  
114 generated southward connections with the Aconcagua Basin and Neuquén Embayment  
115 during this period (Aguirre-Urreta, 2001; Mourgues 2004, Aguirre-Urreta et al., 2007;  
116 Fouquet, 2018).

117 The clastic deposits of Quebrada Monardes Formation (300 to ~1000 m thick) have  
118 been interpreted as transitional to continental environments during Early Cretaceous times,  
119 located at the eastern edge of Chañarcillo Basin, and due to its wide geographical extension  
120 (26-29°S) different paleoenvironments have been described: lagoonal, estuarine, fluvial,

121 alluvial and eolian systems (Muzzio, 1980; Mercado, 1982; Bell and Suárez, 1989; this  
122 paper). This formation conformably overlies shallow marine calcareous sandstones of the  
123 Pedernales and Lautaro formations of Upper Jurassic-Lower Cretaceous ages (Muzzio,  
124 1980; Mercado, 1982; Bell and Suarez, 1989; Cornejo et al., 1998; Mpodozis et al., 2018).  
125 The rocks of the Quebrada Monardes Formation extend for approximately 200 km in a  
126 north-south direction (26°- 28°S and 69°-70° W; Bell and Suárez, 1989) and become  
127 thinner to the west where they probably interfinger with paralic and shallow marine  
128 deposits of the Pabellón, Nantoco and Bandurrias formations which comprise the  
129 Chañarcillo Group. Of these, the Bandurrias Formation represents the volcanic arc located  
130 to the west (Mercado, 1982; Arevalo, 1995).

131         The sparse fossils in the continental red beds of the Quebrada Monardes Formation,  
132 mainly pterosaur fossil bones and dinosaur footprints, have provided no specific ages.  
133 Marine fossils in underlying limestones of the Lautaro and Pedernales Formation and  
134 Quebrada Vicuña strata, indicate a Tithonian-Valanginian age for these successions  
135 (Arevalo, 1995; Mourgues et al., 2015; Mpodozis et al., 2018). However, recent questions  
136 have arisen concerning to the depositional age of this unit. A U-Pb detrital zircon analysis  
137 from a sandstone attributed to the Quebrada Monardes Formation, 105 Km south of Cerro  
138 Tormento gives a value *ca.* 94 Ma maximum depositional date, within the Cenomanian  
139 Stage (Mpodozis et al., 2018). Nevertheless, in the same work a conformable relationship  
140 of the Quebrada Monardes Formation with Lagunillas Formation is accepted, being the last  
141 unit assigned to the late Jurassic-earliest Cretaceous. Therefore, the base of the Quebrada  
142 Monardes Formation would be, at least Early Cretaceous in age.

143

### 144 **1.3 Stratigraphy**

145           The new pterosaur-bearing horizon preserves several disarticulated bones. This  
146 layer corresponds to a 0.7-1.0 m thickness mud clast breccia and sandstone beds (Fig. 2)  
147 intercalated in the upper part of a 160 m thick succession of the Quebrada Monardes  
148 Formation exposed on the eastern flank of Cerro Tormento (4,200 m.a.s.l) in the Atacama  
149 Region, Northern Chile. It is located at 65 km north of the former pterosaur locality of  
150 Cerro La Isla, described by Bell and Suárez (1989), and Martill et al. (2006). This  
151 succession was measured at the eastern flank of Cerro Tormento (4200 m.a.s.l.) and  
152 consists of a set of red to brownish alternation of siliciclastic sandstones, siltstones and  
153 mudstones that reflect deposition in a tidal estuarine environment that overlies limestones  
154 from Pedernales Formation. Principally based on Olariu et al. (2015) five sedimentary  
155 facies and two facies associations were determined.

156

157 ***Facies 1: Laminated mudstones and fine-grained sandstones***

158           Facies 1(F1) represents a mixed sand and mud flat level that includes horizontal to  
159 sub horizontal mm-to cm thick dark purple to reddish mudstones and a minor proportion of  
160 fine-grained sandstones (Fig. 3A) with gradual contacts to Facies 2 and frequent erosive  
161 surfaces at the top. Generally fining upward with rhythmic lamination (varve-type),  
162 desiccation and syneresis cracks, gypsum nodules, rain spots marks and locally horizontal  
163 bioturbations.

164           This facies, dominated by silt, represents a low-energy environment and a low  
165 sedimentary input, where rhythmic lamination was formed through cyclic deposition from  
166 suspension of slack water ponds and sandstones from low-density turbidity currents (Olariu  
167 et al., 2015; Tang et al., 2019). Rain spots, gypsum nodules, desiccation and syneresis  
168 cracks at top of mudstone levels indicate intermittent subaerial exposure (Tucker, 2003;



169 Erin and Arnott, 2007; Boggs, 2009).

170

171 ***Facies 2: Rippled cross-laminated sandstone***

172 Facies 2 (F2) is the dominant facies in Cerro Tormento, consists of unidirectional or  
173 less common bidirectional rippled cross-laminated fine to medium-grained sandstones. The  
174 grains are rounded and well-sorted with an important feldspar and lithic component; cement  
175 is siliceous to lightly calcareous. Rippled cross-laminated sets can be amalgamated,  
176 forming centimetric to decimetric thick beds with normal to reverse grading and  
177 occasionally separated by mm to cm thick mud layers (Fig. 3B). Other structures are flaser  
178 bedding, mud drapes, asymmetrical linguoid ripples and flute casts. F2 is variably  
179 bioturbated, ranging from no burrowing to intense bioturbation with *Planolites* isp. (Fig.  
180 3C).

181 The rippled cross-lamination is interpreted as representing a subtidal or intertidal  
182 relatively low energy environment that can be widespread and unconfined as in an  
183 embayment or in the inner shelf, or confined within a channel (Olariu et al., 2015). The  
184 presence of oppositely directed ripples suggests reversing currents, and mud drapes on  
185 cross bed surfaces (foresets) and flaser bedding indicates periods of low flow velocity or of  
186 slack water in the trough of the dunes during tidal-current reversals (Fig. 2B; Reineck and  
187 Wunderli, 1968; Tucker, 2011; Olariu et al., 2012; Olariu et al., 2015). Local calcareous  
188 cement and variable rates of bioturbation indicate fluctuating salinity and sedimentation  
189 rates. In bioturbated levels (Fig. 3C), there was time for infauna to inhabit and churn Facies  
190 2 (Pemberton et al., 1982; Tang et al., 2019).

191

192 ***Facies 3a: Planar stratified coarse pebbly sandstone***

193 Facies 3a (F3a) consists in planar stratified coarse pebbly sandstone beds (Fig. 3D).  
194 It is present at the lower part of the section and is dominated by centimetric to decimetric  
195 alternations brownish of medium to very coarse-grained sandstones with fine to very fine  
196 feldspar and lithic pebbles and rounded quartz clasts in lag levels. The planar stratification  
197 is continuous and discontinuous in less cases. Beds range from 5 to 20 cm in thickness and  
198 may present normal grading. Flat and erosive top-base contacts and heterolithic  
199 intercalations are common. This facies rapidly upgrades to F4.

200 The relative bigger grain size and pebbly lag levels indicate high hydrodynamic  
201 conditions by strong subaqueous tractive current (Holz, 2003; Plint, 2010; Maahs et al.,  
202 2019), probably reflecting tractional transport during aggradation of longitudinal tidal bars  
203 (Miall, 1977, 1978).

204

205 ***Facies 3b: Mud clast breccia***

206 Facies 3b (F3b) is composed by reddish purple mud clast breccia beds that are 3-25  
207 cm thick (Fig. 3E). This facies is matrix supported (60-55%), matrix is medium to fine  
208 grained sandstone, structureless to planar stratified. Clasts are planar “flakey” shape with  
209 very fine to coarse pebbles size (2-20mm), slightly rounded to angular and locally  
210 imbricated. F3b generally is found an erosional based and is present at various stratigraphic  
211 positions, interbedded with gradual contact to F4. Disarticulated and apparently oriented  
212 pterosaur bones are found in F3b at the top of the section (Figs. 4A and B).

213 This facies is probably indicating reworking of previously deposited, thin, semi-  
214 lithified mud layers from intertidal or supratidal levels by flood tides when high energy  
215 currents agitate sandy sediments and mud clasts, forming high density and turbulent flows  
216 later deposited within tidal bars (Jablonski et al., 2016; Li et al., 2017). The high

217 cohesiveness, “flakey” and angular shape of these clasts suggests minimal transport  
218 distances, due to short periods (few hours) of each flood tide (Musial et al., 2012; Jablonski  
219 et al., 2016; Li et al., 2017). Pterosaur bones were probably transported by the same high  
220 density and turbulent flows, that are likely the result of upstream point bar erosion during  
221 fluvial or tidal flooding periods.

222

#### 223 ***Facies 4: Cross-stratified sandstone***

224 Facies 4 consists of series of upward coarsening units of cross-stratified  
225 unidirectional and bidirectional brownish medium to very coarse-grained sandstones (Fig.  
226 3f) with occasional mud draped foresets (inclined heterolithic stratification) and thin mud  
227 layers (Fig.4C). The cross strata are planar from low to high angle and set thickness range  
228 from 20-50 cm. It presents erosive and rarely channelized bases with load casts or gradual  
229 transitions from F3a and F3b. Calcareous cement and hummocky-like cross stratification in  
230 medium-grained sandstones were identified in few places.

231 Mud draped foresets, deposited during repeated slack water periods, and thick and  
232 orderly stacked sets of cross-stratified sandstones, with uni- and bidirectional paleocurrents,  
233 are believed to be consistent with tidal environments, indicating high energy tidal currents,  
234 probably confined by broad channels (Nio and Yang, 1991; Choi et al., 2004, Longhitano et  
235 al., 2012, Olariu et al., 2015; Tang et al., 2019). No indicators of subaerial exposures have  
236 been observed and most probably these dunes were formed in subtidal conditions. This  
237 facies association is interpreted as being a tidal bar deposit, and each up-coarsening unit is a  
238 single-stage tidal bar (Tang et al., 2019). The local hummocky-like cross-stratification are  
239 result of storm waves erosion (Tucker, 2011).

240

## 241 *Facies Association and Paleoenvironment*

242 With the conjunction and stacking of the previously described facies, two facies  
243 association were determined:

### 244 *Facies Association 1: Muddy heterolithic inter-tidal deposits (tidal plains)*

245 Facies Association 1 (FA1) is composed of intercalated F1 and F2 with wavy  
246 contacts and gradual transitions from F2 to F1. It has 5 to 40 m-thick silt deposits with fine  
247 to medium grained planar and rippled cross laminated sandstones. They are dominantly  
248 normal graded at the top of the section. The ripples are predominantly unidirectional but  
249 throughout the section they migrate in opposite directions. Sandstone beds are cm to dm  
250 thick and sometimes have lenticular like form. Locally presents 1 to 10 cm gypsum filled  
251 nodules.

252 FA1 is interpreted to be formed in an intertidal environment with weak bidirectional  
253 currents (Erin and Arnot, 2007). This environment evolves from aggradational to  
254 progradational at the top. Sand layers are laid down during high-energy ebb or flood tidal  
255 flow, while mud is deposited during low energy slack-water periods in between tidal flows  
256 (Chen et al., 2014). The systematic occurrence of mudstone drapes to mainly unidirectional  
257 ripples suggest a strong tidal influence and deposition in a fluvial channel below the tidal  
258 limit (Tang et al., 2019). Filled gypsum cavities and mud cracks indicated dry and intense  
259 cyclic evaporation periods (Tucker, 2011) between tides, which allows FA1 to be  
260 interpreted as tidal plain deposits (Tucker, 2003; Erin and Arnott, 2007; Boggs, 2009).

261

### 262 *Facies Association 2: Cross stratified tidal sandstone (tidal bars)*

263 Facies Association 2 is mainly composed of F3a, F3b and F4 includes 8-30 m thick  
264 stacked bidirectional and unidirectional cross-stratified sandstones (individual beds 30-70

265 cm thick). The sandstone commonly presents mud drapes and thin mud layers. Local  
266 bioturbations occur in mudstones-wavy sandstone intercalations. The bases are principally  
267 sharp or erosional, usually presenting F3a or F3b. FA2 is dominantly normal graded at the  
268 top.

269 The deposits are interpreted as being tidal bar deposits, and each up-coarsening unit  
270 is a single-stage tidal bar (Tang et al., 2019) within an estuary mouth. The sharp and  
271 erosional bases of F3a, F3b that gradually pass to F4 suggest a broad channelized  
272 environment. Mud clasts breccias (F3b) indicates the erosion of a muddy sediment surface  
273 (tidal plains of FA1) by eddies in a passing turbulent current (Tucker, 2003) carrying them  
274 to the main tidal channel.

275 Observations of the stratigraphy suggest that the accumulation of pterosaur bones  
276 occurred in an estuarine environment, associated to tidal bar deposits, in which the tides  
277 would have had an important influence. It is probable that some specimens died in place or  
278 were carried short distances by the tidal flows, evidenced by the angular mud clasts (Li et  
279 al., 2017), previous to their deposition. Additionally, is possible that loose bones or  
280 specimens showing some degree of association were gradually buried by sediment that was  
281 washed away by the tides, or by river flooding.

282

## 283 **2. MATERIALS AND METHODS**

284 Most of the bones from Cerro Tormento are disarticulated and scattered throughout  
285 the stratum, which includes different parts of the axial and postcranial skeleton. The  
286 specimens are deposited in the Paleontology Area of the Museo Nacional de Historia  
287 Natural of Santiago de Chile (MNHN) under the code SGO.PV. The technical preparation  
288 of some of the fossils from this locality was carried out mechanically in the "Research

289 Workstation” of the MNHN, and in the Laboratory of the Red Paleontológica U-Chile, in  
290 the Faculty of Sciences of the University of Chile.

291

### 292 **3. Systematic paleontology**

293 Pterosauria Kaup, 1834

294 Pterodactyloidea Plieninger, 1901

295 Lophocratia Unwin, 2003

296 Archaeopterodactyloidea Kellner, 1996

297 Ctenochasmatidae Nopcsa, 1928

298 Ctenochasmatidae genus et sp. indet. (Figs. 5-6)

299

300 **Material**— four cervical vertebra of the middle series with the following numbers  
301 collection: SGO.PV.22800, SGO.PV.22801, SGO.PV.22804, SGO.PV.22815.

302

303 **Cervical vertebrae:** SGO.PV.22800 (Fig. 5) is an almost complete three  
304 dimensionally preserved middle cervical vertebra. It is procoelous, with a compressed  
305 neural arch, a little more integrated to the centrum than that observed in the ctenochasmatid  
306 vertebra from Cerro La Isla SGO.PV.350 (Alarcón-Muñoz et al., 2020). The transverse  
307 section of the middle zone of the vertebra is semicircular, with its dorsal surface flattened  
308 and its ventral surface convex. It can be appreciated in anterior view, that the cotyle is  
309 concave, its ventral margin is above the level of the ventral edge of the centrum. The  
310 preexapophyses correspond to rounded protrusions located under the base of the  
311 prezygapophyses; they are convex ventrally and concave dorsally. The anterior opening of  
312 the neural canal has an oval profile, with the horizontal axis greater than the vertical axis,

313 and it is located dorsally with respect to the vertebral centrum. In the anterior section of the  
314 element, well conspicuous ventrolateral grooves arise almost from the base of both  
315 prezygapophyses, which continues posteriorly for approximately a quarter of the length of  
316 the element. The condyle is oval, well developed posteriorly, and is tilted laterally to the  
317 right. The ventral surface of the condyle is convex, while the dorsal surface is a little more  
318 flattened. The lateral surfaces of the condyle are approximately flattened and open slightly  
319 laterally. In ventral view, it is appreciated that the condyle arises from the vertebral centrum  
320 as ridges on both sides that separate like wings, diverging until reaching the  
321 postexapophysis. The postexapophyses are well preserved, especially the left, and they  
322 protrude from the condyle as small “rounded wings”. Their articular surfaces are low and  
323 integrated with the condyle. In dorsal view, the neural spine was not preserved due to the  
324 erosion to which the vertebra was exposed. As a result, the filling of the neural canal is  
325 exposed, especially in the anterior half. The neural canal is approximately tubular.

326         The prezygapophyses and postzygapophyses of SGO.PV.22800 are well preserved  
327 and practically complete, except for the left prezygapophysis, which only retains its base.  
328 The right prezygapophysis is well developed, it exceeds anteriorly the level of the cotyle  
329 and is oriented laterally about  $15^\circ$  with respect to the main axis of the vertebra and rises  
330 slightly dorsally. The prezygapophyses show little lateral divergence and hardly rise  
331 dorsally, not exceeding the dorsal edge of the neural canal. The articular surface of the  
332 prezygapophysis is flattened and is directed dorsomedially. The postzygapophyses show  
333 great development, and do not exceed the posterior border of the condyle. The  
334 postzygapophyses are oriented dorsolaterally at an angle of about  $30^\circ$  with respect to the  
335 longitudinal axis of the vertebral centrum. The articular surfaces of the postzygapophyses  
336 are flat, oval in outline, and oriented ventromedially. In the ventral surface, the

337 hypapophysis is observed, which is poorly preserved. The hypapophysis corresponds to a  
338 faint ridge that extends posteriorly from the cotyle to approximately one fifth of the  
339 element's extension. Due to deformation of the vertebra, the hypapophysis is displaced to  
340 the left. At this point, the hypapophysis is conspicuously protruding from the ventral edge  
341 of the vertebra. In its general dimensions, SGO.PV.22800 is less robust than the two  
342 vertebrae of ctenochasmatids from Cerro La Isla (Alarcón-Muñoz et al., 2020), being  
343 narrower in dorsal view and lower in lateral view.

344 Specimen SGO.PV.22801 (Fig. 6A-B) corresponds to a middle cervical vertebra  
345 preserved in two slabs. One of the slabs retains most of the element in dorsal view, while  
346 the other retains mostly its mold. SGO.PV.22801, like the other mid cervical vertebrae  
347 from Cerro Tormento, is elongated. It has a well-developed posterior condyle, which is  
348 quite expanded mediolaterally. The presence of postexapophyses integrated in the condyle  
349 is not clearly distinguished due to its poor state of preservation. The postzygapophyses are  
350 also not preserved. In dorsal and ventral view, the vertebral centrum has concave lateral  
351 surfaces, giving the vertebra an “hourglass” appearance. Because the vertebra lacks its  
352 midsection, the impression of the ventral surface is visible. A well-developed hypapophysis  
353 is observed, extending to at least the middle of the element. From posterior to anterior, the  
354 vertebra progressively expands mediolaterally, culminating in the prezygapophyses. Part of  
355 the left prezygapophysis is especially evident, which diverges slightly laterally, like  
356 SGO.PV.22800. In the impression of the dorsal surface of the vertebra, and in its anterior  
357 portion, it is possible to observe the impression of the neural spine. This impression has a  
358 constant depth throughout the entire visible section (approximately 3 mm), which leads to  
359 the interpretation of a neural spine of relatively constant height, at least in that section.



360 Specimen SGO.PV.22804 (Fig. 6C) corresponds to a middle cervical vertebra  
361 represented only by the preserved posterior half in ventral view, while the rest of the  
362 element is preserved as the impression of its dorsolateral surface. The vertebra is elongated,  
363 its ends are expanded, and its lateral margins are concave, giving the vertebra an  
364 “hourglass” shape. The preserved portion of the vertebral centrum has an approximately  
365 tubular cross section, although its ventrolateral surfaces are almost flat. In the impression of  
366 the anterior portion, it is possible to see part of the neural spine, partially preserved as bone  
367 tissue embedded in the matrix and partially as an impression. It is difficult to elucidate its  
368 morphology, although it can be noted that the neural spine was long and low. Only the  
369 impression of the base of the right prezygapophysis is preserved, which is latero-anteriorly  
370 directed. The condyle is well developed, and its lateral margins were apparently straight,  
371 while its articular surface shows a closely convex profile. Judging from the preserved  
372 impressions, the postzygapophyses were elongated and projected posterolaterally. Unlike  
373 all the other vertebrae, this element is considerably small (see Table 1).

374 Specimen SGO.PV.22815 (Fig. 6D) corresponds to the anterior portion of a middle  
375 cervical vertebra. Only the left prezygapophysis is preserved, which is robust and projected  
376 anteriorly, with a slight lateral displacement. Its lateral border is slightly convex while its  
377 medial border is concave and continues with the anterior border of the neural arch. The  
378 prezygapophysis has a medially oriented, rounded articular surface at its anterior end, with  
379 a slight dorsal orientation. The right lateral border of the neural arch is slightly concave and  
380 forms a lateral ridge that marks the boundary with the vertebral centrum. The neural spine  
381 is partially preserved. This begins approximately 0.5 cm from the anterior border of the  
382 neural arch. The preserved section of the neural spine is low and maintains a relatively  
383 constant height.

384

385 **Comparisons.**

386 Kellner (2003) proposed that elongated middle cervicals, but not to the same degree  
387 as in the Azhdarchidae, with low neural spines, are synapomorphies of the  
388 Archaeopterodactyloidea. This clade contains the Germanodactylidae and  
389 Euctenochasmatia, a group that in turn contains *Pterodactylus*, *Ardeadactylus* and  
390 Ctenochasmatoidea, which contains the Gallodactylidae and Ctenochasmatidae (Andres  
391 and Myers, 2013). A similar opinion is expressed by Unwin (2003), who mentioned that  
392 elongated cervical vertebrae with depressed neural arches and low, rectangular neural  
393 spines are diagnostic features of Euctenochasmatia.

394 Elongated vertebrae, with low, rectangular neural spines, and compressed neural  
395 arches are present especially in the clade Ctenochasmatidae. This group includes species  
396 such as *Gegepterus changae* Wang et al., 2007, *Elanodactylus prolatus* Andres and Ji,  
397 2008, *Pterodaustro guinazui* Bonaparte, 1970, *Beipiaopterus chenianus* Lü, 2003,  
398 *Ctenochasma taqueti* Bennett, 2007, *Eosipterus yangi* Ji and Ji, 1997, and *Huanhepterus*  
399 *qingyangensis* Dong, 1982, which are characterized by having long compressed snouts,  
400 with fine, very closed spaced teeth.

401 A similar morphology to that described in vertebrae of the Ctenochasmatidae is  
402 observed in the Azhdarchidae, although in this group the neural arch is completely  
403 confluent with the vertebral centrum, forming a single tubular structure (Buffetaut et al.,  
404 1997; Martill et al., 1998; Unwin, 2003; Andres and Ji, 2008, Rodrigues et al., 2011;  
405 Buffetaut, 2012). As in the Ctenochasmatidae, the neural arch of the vertebrae of pterosaurs  
406 from Cerro Tormento, although depressed, remains distinguishable from the vertebral  
407 centrum (Unwin, 2003; Andres and Ji, 2008). Additionally, the elongation of the vertebrae

408 from Cerro Tormento is not as marked as that described in the Azhdarchidae. In some  
409 azhdarchids such as *Quetzalcoatlus lawsoni* Andres and Langston, 2021, and  
410 *Arambourgiania philadelphiae* Arambourg, 1954, the cervical vertebrae are  
411 hyperelongated, with minimum centrum length / width ratios close to 12 in some species  
412 (Frey and Martill, 1996; Witton, 2007).

413         One feature observed in specimen SGO.PV.23800 that suggests that it belongs to a  
414 ctenochasmatid is the position of the neural canal. Martill et al. (2013) mentioned that in  
415 the Azhdarchidae the neural canal is centrally positioned, unlike the Ctenochasmatidae. In  
416 the specimen SGO.PV.22800, the neural canal is dorsally positioned, which contrasts with  
417 that described in the Azhdarchidae by Martill et al. (2013).

418         The cervical vertebrae of Cerro Tormento are procoelous, elongated, and with  
419 depressed neural arches. Some of them preserve evidence of a low and elongated neural  
420 spine. Its global morphology is like two middle cervical vertebrae attributed to the  
421 Ctenochasmatidae from Cerro La Isla (Alarcón-Muñoz et al., 2020). Like the middle  
422 cervical vertebrae of Cerro La Isla, the middle cervical vertebrae are elongated, and the  
423 neural arch is well integrated into the vertebral centrum. In addition, with the vertebrae of  
424 Cerro La Isla, in the SGO.PV specimen, it is appreciated that the neural arch is located  
425 dorsally, and not centralized, as in the Azhdarchidae. The fact that the cervical vertebrae of  
426 both localities coincide in morphology and in the geological unit of origin, suggests that the  
427 vertebrae of Cerro Tormento also belong to ctenochasmatids, and perhaps also the same  
428 species.

429

430 Archaeopterodactyloidea indet. (Figs. 7-10)

431

432 **Materials**—SGO.PV.22805, impression of a right scapulocoracoid associated with an  
433 incomplete tibiotarsus impression; SGO.PV.22810, left coracoid; SGO.PV.22806,  
434 impression of incomplete left humerus; SGO.PV.22807, distal portion of a left humerus  
435 preserved in a slab. SGO.PV.22808, distal section of right humerus; SGO.PV.22814,  
436 incomplete impression of the left femur.

437

438 **Scapulocoracoid.** Specimen SGO.PV.22805 (Fig. 7A) corresponds to a sandstone  
439 slab that preserves almost complete impression of a right scapulocoracoid in lateroventral  
440 view. A cast from the impression of the scapulocoracoid was made, which allowed a better  
441 description of this element (Fig. 7A). The scapula lacks the medial end. Its diaphysis is  
442 elongated and narrow, slightly curved and compressed dorsoventrally, with a thicker  
443 dorsolateral rim. The lateral end of the scapula is expanded, convex and it forms the  
444 posterior and dorsal part of the glenoid fossa, with a slightly sub-triangular shape; this  
445 expansion is named here as a supraglenoid process. In *Pteranodon* this process is called  
446 supraglenoid buttress (Bennett, 2001). In addition, the lateral end of the coracoid is also  
447 expanded, robust, and forms the ventral region of the glenoid fossa. This thickening is  
448 named here the coracoid process.

449 Although the coracoid process is incomplete, its preserved portion suggests that it  
450 was more prominent than the supraglenoid process. The glenoid fossa remains almost  
451 complete, only lacking its most dorsal edge. The articular surface of the glenoid fossa is  
452 markedly concave, and it is saddle-shaped, a morphology that extends to its ventral edge,  
453 without the presence of any appreciable ridge. There is no evidence of a suture in the  
454 glenoid fossa separating the scapula from the coracoid. The coracoid lacks its medial end,  
455 the section that articulated with the sternum. The coracoid has a more robust constitution

456 than the scapula. Its shaft is elongated, straight, and compressed anteroposteriorly, with a  
457 marked ventral ridge. The diaphysis expands anteriorly, separated some distance from the  
458 coracoid process, developing a marked procoracoid (Wellnhofer, 1991). Distally, from the  
459 procoracoid, there is a small tubercle.

460 Specimen SGO.PV.22810 corresponds to a left coracoid (Fig. 7B-E), is  
461 dorsoventrally compressed, and the preserved length is 57 mm. The ventral surface (F) is  
462 almost flat, while the dorsal surface (C) is proximally flat and distally concave. The medial  
463 end of the coracoid that forms part of the glenoid fossa is robust, anteroposteriorly  
464 expanded, and concave in the center. The last feature is marked as coracoidal glenoid cavity  
465 in the specimen. The coracoidal tubercle is eroded. The shaft is anteroposteriorly narrow  
466 and slightly sigmoidal in its mid zone. The articular surface for the sternum (asfs)  
467 corresponds to the medial end; it is anteroposteriorly wide with respect to the total length  
468 of the element, with a well-marked posterior expansion. This articular surface for the  
469 sternum is dorsoventrally narrow and proximally convex, with a concavity in the midpoint.

470

471 **Comparisons.** In adult pterosaurs, the scapula and coracoid fuse late in ontogeny  
472 and form a single bone, which can be V or U-shaped (Bennett, 2001; Wellnhofer, 1975).  
473 Complete fusion of skeletal elements is one of the criteria proposed by Bennett (1993) to  
474 identify osteologically mature individuals. The absence of any suture signal between the  
475 scapula and the coracoid suggests that SGO.PV.22805 probably belonged to a mature  
476 individual, although this is difficult to ascertain from an impression. The glenoid fossa in  
477 SGO.PV.22805 is oriented anterolaterally, a feature that is proposed by Romer (1956) as a  
478 synapomorphy of the Pterosauria.

479           The morphological differences of the glenoid fossa of non-pterodactyloids and  
480 pterodactyloids appear to be related to the amplitude of movement of the humerus, which in  
481 turn is directly related to the morphology of the distal end of this element (Fujiwara and  
482 Hutchinson, 2012; Witton, 2015). In the Pterodactyloidea, the morphology of the glenoid  
483 fossa is described as "symmetric", since its dorsal and ventral articular surfaces are similar,  
484 and the latter does not present a ventral crest that limits the abduction of the humerus to a  
485 subvertical position, as in non-pterodactyloids (Witton, 2015). The morphology of the  
486 glenoid fossa provides clues about the posture of the forelimbs of a pterosaur when moving  
487 on land. This morphology allowed the pterodactyloids to acquire upright postures of the  
488 forelimbs when walking on land (Witton, 2015). The morphology of the glenoid fossa of  
489 SGO.PV.22805 is clearly symmetrical, without the presence of a prominent ridge on the  
490 ventral articular surface. Thus, this material is referred to the Pterodactyloidea based on its  
491 relatively large dimensions and in that the glenoid fossa is shared equally by the scapula  
492 and the coracoid. In contrast, in non-pterodactyloids the glenoid cavity is located mostly or  
493 completely on the scapula (Wellnhofer, 1975). Likewise, the scapulocoracoid  
494 SGO.PV.22805, is similar to the scapulocoracoid of *Pterodaustro* (L.C. pers. obs), as in  
495 that pterosaurs, apparently the two bones in SGO.PV.22805 are similar in length  
496 (subequal).

497

498           **Humerus.** Specimen SGO.PV.22806 (Fig. 8A) corresponds to the impression of an  
499 almost complete left humerus preserved next to the shaft of an indeterminate long bone  
500 (from the curvature it would seem an incomplete femur). A portion of the proximal end of  
501 the humerus is expanded with respect to the shaft, which corresponds to the impression of  
502 the deltopectoral crest. This structure curves anteroventrally, seems to be D-shaped and

503 probably occupies approximately 30% of the length of the diaphysis. From the  
504 deltopectoral crest to the distal end, the element tapers very slightly, continuing in an  
505 approximately straight diaphysis, then gradually expanding again as it approaches the distal  
506 end. The distal end of the impression is markedly expanded with respect to the shaft,  
507 unfortunately no diagnostic morphological characters can be observed in this specimen, but  
508 they are preserved in other two fossils.

509 A distal portion of a left humerus (SGO.PV.22807, Fig. 8B) is exposed in  
510 posterodorsal view. The diaphysis is distorted, slightly sigmoidal and of approximately  
511 constant diameter in the preserved portion, culminating in a distal epiphysis that is  
512 especially expanded laterally.

513 Specimen SGO.PV.22808 (Fig. 9) corresponds to the distal end of a right humerus,  
514 very well preserved and almost tridimensional, with a sinuous distal edge. In anterior view,  
515 the distal epiphysis is greatly expanded with respect to the diameter of the diaphysis, an  
516 expansion that is given by the great development of the ectepicondyle and the  
517 entepicondyle. The ectepicondyle has a subtriangular profile and is elevated relative to the  
518 level of the distal surface of the element, with its articular surface facing slightly anteriorly.  
519 The ectepicondyle limits a wide, but not very deep concavity restricted in the lateral half of  
520 the epiphysis, which extends to the edge of the distal end. The entepicondyle is less  
521 developed than the ectepicondyle. It has a rounded or elongated profile and is separated  
522 from the rest of the element by a groove that runs longitudinally along the proximo-distal  
523 axis of the bone, and it is deeper distally.

524 The trochlea (medial condyle) is partially eroded, and it is observed in anterior  
525 view, its profile is oval, with the lateral-medial axis longer than the proximal-distal one.  
526 The capitulum (lateral condyle) is oriented distally, it is oval shaped, with its most distal

527 edge rounded. The capitulum and trochlea are separated by a well-marked intercondylar  
528 groove. In posterior view, expansion of the distal epiphysis is also evident; the  
529 entepicondyle shows the same rounded profile as in anterior view, and the ectepicondyle is  
530 conspicuously curved anteriorly. The dorsal edge of the bone is flattened along its entire  
531 length, while the ventral edge is concave. In distal view, SGO.PV.22808 has a  
532 subrectangular profile. Its posterior border is slightly convex, while the anterior border is  
533 slightly sinuous, although with a slight flattened elevation in its medial half, which is  
534 separated from the entepicondyle by the terminal of the sulcus that is described in anterior  
535 view. The entepicondyle sulcus is observed to be slightly displaced anteriorly. The  
536 subtriangular profile of the ectepicondyle is also observed, with its apex located well  
537 anteriorly and its lateral border obliquely in relation to the anteroposterior axis.

538

539 **Comparisons.** An expanded proximal humerus head (saddle-shaped) with a broad  
540 deltopectoral crest correspond to proposed synapomorphies for the Pterosauria (Romer,  
541 1956; Wellnhofer, 1978). The deltopectoral crest has proven to be of systematic value in  
542 pterosaur phylogenies (Unwin, 2003). Unfortunately, in the only specimen that retains part  
543 of the deltopectoral crest (SGO.PV.22806), this structure is too incomplete for detailed  
544 comparisons. However, some conclusions can be drawn that would allow us to specify in a  
545 general way the systematic position of the pterosaur to which the humerus belonged.  
546 According to Kellner (1996), among pterodactyloids the deltopectoral crest has 3 types of  
547 basic morphology. The first type corresponds to deltopectoral crests that are located  
548 proximally and that are curved ventrally. This morphology is common in  
549 archeoptero-dactyloid and tapejaroid pterosaurs, which according to Kellner (1996), differs  
550 from that of all non-pterodactyloids. Examples of humeri with this deltopectoral crest



551 morphology are observed in *Beipiaopterus chenianus* (Lü, 2003), the gallodactylid  
552 *Gallodactylus suevicus*, the pterodactylids *Pterodactylus kochi* (Wellnhofer, 1978) and  
553 *Pterodaustro guinazui* (Codorniu and Gasparini, 2007; fig. 1 in Codorniu et al., 2013). The  
554 second type is a distally displaced “hatchet-shaped” deltopectoral crests, a morphology that  
555 is characteristic of the Nyctosauridae (Kellner, 1991; 2003). This morphology of the  
556 deltopectoral crest is similar to that present in the Rhamphorhynchidae, but in them the  
557 deltopectoral crest is more proximally displaced (Kellner, 2003). The third type is the  
558 “warped” deltopectoral crests, typical of the clade Pteranodontoidea. A good example of  
559 this is the humerus of *Istiodactylus* (formerly *Ornithodesmus*) *latidens*, in which the  
560 deltopectoral crest practically rotates over the ventral surface of the bone (Hooley, 1913;  
561 Wellnhofer, 1978; Bennett, 1989). The deltopectoral crest of *Hatzegopteryx thambema*  
562 (Buffetaut et al. 2002) is much more developed; its upper and lower edges form a right  
563 angle with respect to the longitudinal axis of the diaphysis. Judging by the visible portion in  
564 the Chilean specimen (SGO.PV.22806), the morphology of the deltopectoral crest does not  
565 agree with that observed in the Rhamphorhynchidae or Nyctosauridae (Wellnhofer, 1975,  
566 1978; Kellner, 1991, 2003; Padian, 2008; Andres et al., 2010), and also differs from that  
567 present in the Azhdarchidae.

568         The new specimens SGO.PV.22807 and SGO.PV.22808, show some features with  
569 informative value for the resolution of their systematic position. These fragments of the  
570 distal end of the humerus show an expanded distal epiphysis in relation to the diaphysis,  
571 due to the great development of the ectepicondyle and entepicondyle (principally the  
572 ectepicondyle), while their condyles (capitulum and trochlea) are proportionally reduced  
573 (SGO.PV. 22808). The great expansion of the distal portion of the humerus with respect to  
574 the diaphysis, due to the great development of the ectepicondyle and entepicondyle, and

575 with underdeveloped condyles, constitutes a well-extended feature in the Pterodactyloidea  
576 (Fujiwara and Hutchinson, 2012; Witton, 2015). Fujiwara and Hutchinson (2012) describe  
577 a close relationship between the morphology of the distal humerus and the posture of the  
578 forelimbs in extant quadrupeds. These authors found a very close relationship between the  
579 degree of expansion of the distal end of the humerus, the degree of development of the  
580 condyles, and the posture they maintained when moving on land. It was found that  
581 expanded distal humerus ends with little development of the condyles seem to be related to  
582 upright postures of the forelimbs when walking on the ground, a feature that would  
583 characterize most pterodactyloids, while reduced distal humerus ends, with little  
584 development of the ectepicondyle and entepicondyle and great development of the condyles  
585 would be related to a more open posture of the forelimbs during their displacement on land,  
586 a trait that would characterize most non-pterodactyloids (Witton, 2015).

587         The morphology of SGO.PV.22808 agrees with what can be observed in members  
588 of the Pterodactyloidea, which also suggests that in life the extremities of this pterosaur  
589 would have remained upright during its movement on land. This type of morphology  
590 indicates a greater predominance of habits that imply movement on land, a characteristic  
591 that seems to have been well extended in the members of the clade Lophocratia, which  
592 includes pterosaurs for which a greater degree of activity in the terrestrial environment is  
593 inferred than those that integrate other more basal clades (Witton, 2013).

594         Bennett (2001) mentioned the shape of the distal epiphysis of the humerus as being  
595 of diagnostic value. Bennett (2001) and Kellner (2003) propose as a diagnostic feature of  
596 the clade Pteranodontoidea the subtriangular shape of the distal epiphysis of the humerus  
597 when observed in distal view. According to these authors, this morphology differs from the  
598 “D”, oval or rectangular shape found in azhdarchoids. A similar proposal is made by Unwin

599 (2003). He proposes that the triangular contour of the distal epiphysis in distal view is  
600 diagnostic for the clade Ornithocheiroidea, which is defined by this author as the most  
601 recent common ancestor of *Istiodactylus latidens* and *Pteranodon longiceps* plus all their  
602 descendants, and which includes a *Istiodactylus*, Ornithocheiridae, Pteranodontidae and  
603 *Nyctosaurus*. In contrast, Unwin (2003) mentions that in non-Ornithocheiroid pterosaurs  
604 the profile of the distal end is subrectangular or has a “D” shape. The distal view of  
605 SGO.PV.22808 clearly shows a subrectangular to D-shaped profile, which suggests ruling  
606 out the inclusion of the pterosaur to which this humerus belonged in the clade  
607 Pteranodontoidea proposed by Kellner (2003) and in the clade Ornithocheiroidea proposed  
608 by Unwin (2003).

609         The great expansion of the distal epiphysis and the very reduced condyles in  
610 relation to this expansion make it possible to assign SGO.PV.22808 to the  
611 Pterodactyloidea, while the non-triangular shape of this element in distal view makes it  
612 possible to rule out its inclusion in the Pteranodontoidea clade defined by Kellner (2003)  
613 and in the Ornithocheiroidea clade defined by Unwin (2003). This suggest the possibility  
614 open that SGO.PV.22808 belongs to a pterosaur of the clade Archaeopteroactyloidea.

615

616         **Femur.** Bone and impression of much of the anterior surface of a left femur is  
617 preserved in two blocks (SGO.PV.22814, Fig. 10). A cast from the impression of the femur  
618 was made, which allowed a better description of this bone. The specimen consists of the  
619 proximal end, almost complete shaft, and lacks the distal epiphysis. The total length  
620 preserved is about 9 cm. The shaft of the femur expands laterally from approximately one  
621 third of the length of the element in other pterosaurs (Young, 1964; Bonaparte, 1970;  
622 Kellner and Tomida, 2000). This lateral expansion is not evident in the preserved shaft of

623 SGO.PV.22814. Based on this observation, the element lacks approximately one third of its  
624 total length, and the estimated total length is around 14 cm. The proximal end shows a well-  
625 developed femoral head, with a diameter greater than that of the diaphysis, with a rounded  
626 convex articular surface, with a dorsomedial orientation. The femoral neck is short and  
627 wide, and constricted in the middle. The approximate diameter in the narrowest area of the  
628 femoral neck is 70% of the diameter of the femoral head. The orientation of the femoral  
629 head with respect to the longitudinal axis of the shaft (specifically with respect to its medial  
630 surface) is approximately  $130^\circ$ . The diaphysis curves slightly medially and to a lesser  
631 extent anteriorly, and practically does not vary in diameter in the preserved section. The  
632 external trochanter, also called the great trochanter or greater trochanter (Bennett, 2001) is  
633 well developed, projects dorsomedially but does not exceed the median constriction of the  
634 femoral neck. Its shape is subrectangular, with its blunt proximal end. The external  
635 trochanter arises from the lateral surface, slightly below the level of the base of the femoral  
636 neck, continuing proximally obliquely with respect to the longitudinal axis of the diaphysis  
637 as a crest, which protrudes anteriorly. The external trochanter of SGO.PV.22814, as in most  
638 pterosaurs, gradually fuses distally into the diaphysis (Rauhut et al. 2017). It is not possible  
639 to observe the internal trochanter or the presence of any foramen on the intertrochanteric  
640 surface because there is a fracture in this zone.

641

642 **Comparisons.** In general, the femora of non-pterodactyloid pterosaurs are  
643 characterized by having straight shafts (Kellner, 1996). This can be seen in the femur of  
644 *Campylognathoides zitteli* (Plieninger, 1894; Wellnhofer, 1978), *Dorygnathus banthensis*  
645 (Theodori, 1852; Wellnhofer, 1978) and *Rhamphorhynchus muensteri* (Wellnhofer, 1975,  
646 1978). In contrast, in the Pterodactyloidea the diaphysis is usually curved antero-medially,

647 although the degree of curvature varies according to the species (Kellner, 1996). Examples  
648 of pterodactyloids with antero-medially curved shaft include *Pteranodon* (see Eaton, 1910;  
649 Wellnhofer, 1978; Bennett, 1991, 2001), *Nyctosaurus gracilis* (see Williston, 1903),  
650 *Dsungaripterus weii* Young, 1964, and *Herbstosaurus pigmaeus* Casamiquela, 1975.  
651 However, the pterodactyloid *Istiodactylus latidens* (previously *Ornithodesmus latidens*) has  
652 a femur whose diaphysis is quite straight, unlike the other pterodactyloids mentioned  
653 (Hooley, 1913; Wellnhofer, 1978). Relatively straight diaphyses are also observed in the  
654 femora of *Pterodactylus longicollum* (see Wellnhofer, 1970, 1978) and *Gallodactylus*  
655 *suevicus* (see Plieninger, 1907; Wellnhofer, 1978), although in the former the diaphysis  
656 presents a slight antero-medial curvature. The diaphysis of SGO.PV.22814 is slightly  
657 curved medially, and to a lesser degree anteriorly, in agreement with what is observed in  
658 most of the pterodactyloids. The shaft of the femur of *Anhanguera piscator* is slightly  
659 straighter than that of SGO.PV.22814 (Kellner and Tomida, 2000). On the other hand, the  
660 shaft of the femur of *Dsungaripterus weii* curves both anteriorly and medially more  
661 markedly than in SGO.PV.22814 (Young, 1964). In the femur of *Pterodaustro guinazui*  
662 there is also a noticeable anterior curvature (Bonaparte, 1970; Codorniu et al., 2013). The  
663 marked curvature of the femur in two planes (both anteriorly and medially) has been cited  
664 as a diagnostic characteristic of the Dsungaripteridae (sensu Unwin, 2003), a proposal made  
665 mainly based on observations made in *Dsungaripterus weii* (Unwin, 2003; Fastnacht,  
666 2005). However, this bidirectional curvature of the femur is also observed in other  
667 pterosaurs, such as *Dimorphodon* (see Padian, 1983), and in the pterodactyloid femurs  
668 mentioned above. This suggests that this trait is actually widespread among pterosaurs,  
669 especially among pterodactyloids (Unwin, 2006).

670           The shape of the femoral neck and head, together with their orientation with respect  
671 to the shaft, allow, to some extent, to discriminate between the different forms of known  
672 pterosaurs. Constrained necks that separate the femoral head from the rest of the element is  
673 a typical characteristic in pterosaurs, being proposed as a synapomorphy of the Pterosauria  
674 (Kellner, 1996; Kellner and Tomida, 2000). Among femora of non-pterodactyls,  
675 SGO.PV.22814 differs from that of *Campylognathoides zitteli* in that in the latter the  
676 femoral head is oriented at a greater angle with respect to the diaphysis and there is  
677 practically no difference between the diameter of the head and of the femoral neck  
678 (Plieninger, 1894; Wellnhofer, 1978). SGO.PV.22814 differs from the femur of  
679 *Dorygnathus banthensis* in that the proximal portion of the element (from which the  
680 femoral head arises) is bulbous, and narrows distally, giving rise to a straight diaphysis  
681 (Theodori, 1852; Wellnhofer, 1978). In contrast, SGO.PV.22814 does not present this  
682 bulbous of the proximal portion, but rather continues distally in a slightly curved diaphysis  
683 with a relatively constant diameter. SGO.PV.22814 also differs from the femur of  
684 *Rhamphorhynchus muensteri* in that in this species there is little differentiation between the  
685 head and the femoral neck, not presenting a markedly constricted neck (Wellnhofer, 1975).  
686 Regarding pterodactyls, SGO.PV.22814 differs from the femur of *Caiuajara dobruskii*  
687 (Azhdarchoidea, Tapejaridae) in that it has a proportionally longer, unconstrained, and  
688 more dorsally oriented femoral neck, and the external trochanter projects more dorsally,  
689 generating a more marked concavity between it and the dorsal surface of the femoral neck.  
690 These traits remain uniform throughout the ontogeny of this animal (Manzig et al., 2014).  
691 The femora of azhdarchids (Azhdarchoidea, Azhdarchidae) are poorly understood  
692 (Buffetaut et al., 2002), so making comparisons with members of this group is more  
693 complicated. For example, *Azhdarcho lancicollis* (see Nesson, 1984; Averianov, 2010)

694 only conserves the proximal portion of the femur. This, unlike SGO.PV.22814 has a much  
695 narrower and elongated neck, with a constant thickness throughout its length, oriented at a  
696 much greater angle with respect to the diaphysis, as is characteristic of the clade  
697 Ornithocheiroidea (see discussion below) ending in a proportionally much smaller head,  
698 and also has a higher and sharper greater trochanter (see Averianov, 2010). On the other  
699 hand, the femur of *Zhejiangopterus linhaiensis* (M1323) is almost completely known, but  
700 few features are distinguishable in the femur illustrated in Cai and Wei (1994), although  
701 there are notable differences with SGO.PV.22814, mainly in its proximal portion. The  
702 femoral neck in *Zhejiangopterus linhaiensis* is proportionally shorter and is not constricted,  
703 but in anterior view its sides are approximately parallel, and also the angle between the  
704 femoral head and the diaphysis is greater, being markedly directed dorsally, as is common  
705 in the Ornithocheiroidea (Unwin, 2003). SGO.PV.22814 differs from the femur of  
706 *Anhanguera piscator* in that in this species there is less difference between the diameter of  
707 the femoral head and the femoral neck (Kellner and Tomida, 2000). A developed  
708 “mushroom-shaped” femoral head with a narrow neck has also been described in  
709 *Dsungaripterus weii*, a member of the Dsungaripteridae (Fastnach, 2005). However, in this  
710 species the femoral neck is proportionally longer than in SGO.PV.22814. In Chile, remains  
711 of a specimen belonging to the Dsungaripteridae have been recorded, which was given the  
712 name *Domeykodactylus ceciliae* by Martill et al. (2000). However, the femur of this species  
713 is unknown, and it is not possible to make comparisons. This morphology is also observed  
714 in the femur of the pterodactyloid *Herbstosaurus pigmaeus* (see Casamiquela, 1975), a  
715 pterosaur found in the Vaca Muerta Formation (Upper Jurassic, Tithonian), whose femoral  
716 neck appears to be shorter than in *Dsungaripterus weii*, keeping a greater similarity with  
717 SGO. PV.22814. The femur from Cerro Tormento bears a remarkable similarity with a

718 femur not yet formally described referred to in cf. *Ardeadactylus* sp., figured in Rauhut et  
719 al. (2017), specifically in the morphology of the proximal epiphysis. As in SGO.PV.22814,  
720 this femur has a mushroom-shaped head separated from the diaphysis by a relatively short  
721 neck and constricted in its middle area. In addition, the femur of cf. *Ardeadactylus* sp. has a  
722 similar morphology and separation between the external trochanter and the lateral  
723 tuberosity. In the opinion of Rauhut et al. (2017), this femur probably belongs to the  
724 species *Ardeadactylus longicollum*, which is part of the clade Archaeopterodactyloidea  
725 (Bennett, 2012).

726         The angle between the femoral head and the diaphysis of SGO.PV.22814 ( $130^\circ$ ) is  
727 another useful feature to elucidate its relationship with other pterosaurs. In *Herbstosaurus*  
728 *pigmaeus* Casamiquela, 1975, and in the archaeopterodactyloid *Wenupterix uzi* Codorníu  
729 and Gasparini, 2013, from the Tithonian of Neuquén, the femoral neck and head are  
730 directed medially with an angle of approximately  $100^\circ$  with respect to the main axis of the  
731 diaphysis (Codorníu et al., 2006; Codorníu and Gasparini, 2013). This difference separates  
732 the femora of these pterodactyloids from the femora of the pterosaurs belonging to the  
733 clade Ornithocheiroidea sensu Unwin (2003), since an angle between the femoral neck and  
734 the diaphysis of the femur that exceeds  $160^\circ$  corresponds to a synapomorphy of this clade  
735 (Unwin and Lü, 1997; Unwin, 2003). Derived non-pterodactyloids and non-ornithocheiroid  
736 pterodactyloids (the Ornithocheiroidea sensu Unwin, 2003) have a constricted femoral neck  
737 and a dorsomedially directed femoral head (caput) at an angle of approximately  $135^\circ$  with  
738 respect to the longitudinal axis of the diaphysis. This angle is interpreted as a plesiomorphic  
739 trait for pterodactyloids, while in ornithocheiroids (sensu Unwin, 2003) the femoral neck is  
740 relatively robust and markedly directed dorsally at an angle of about  $160^\circ$  with respect to  
741 the diaphysis. Examples of ornithocheiroids with separation angles between the femoral



742 neck and the diaphysis of values greater than  $160^\circ$  are *Anhanguera piscator* (see Kellner  
743 and Tomida, 2000), *Pteranodon* (see Eaton, 1910; Wellnhofer, 1978; Bennett, 1991, 2001),  
744 *Nyctosaurus gracilis* (see Williston, 1903; Wellnhofer, 1978), *Istiodactylus latidens* (see  
745 Hooley, 1913; Wellnhofer, 1978), *Zhejiangopterus linhaiensis* (according to the illustration  
746 of the femur in Cai and Wei, 1994) and *Azhdarcho lancicollis* (see Nessov, 1984;  
747 Averianov, 2010).

748 SGO.PV.22814 is referred to the Archaeopterodactyloidea principally based on the  
749 angle between the femoral neck and the shaft less than  $160^\circ$ .

750

751 Pterodactyloidea indet. (Figs. 11)

752

753 **Materials**—SGO.PV.22805, partial impression of a left tibiotarsus associated with the  
754 impression of a scapulocoracoid.

755

756 **Tibiotarsus.** Specimen SGO.PV.22805 (Fig. 11) correspond to the impression of  
757 the distal end and part of the shaft of a left tibiotarsus in anterior view, associated with the  
758 impression of a scapulocoracoid. The shaft presents a slight curvature in the anteromedial  
759 direction. The distal epiphysis is expanded and appears to be slightly rotated laterally. In  
760 addition, the anterior surface of the lateral and medial condyle can be appreciated. The  
761 lateral condyle shows a great development with respect to the diaphysis, with its proximal  
762 end rounded. The medial condyle, although incomplete, shows less development than the  
763 lateral condyle, forming a slightly concave rim medially. Between the medial and lateral  
764 condyles is a wide, shallow intercondylar groove.

765 **Comparisons.** The tibia in pterosaurs presents few informative features (Kellner,

766 2003; Unwin, 2003). In complete specimens, the most important features are related to the  
767 relative proportions with respect to the femur, although this only serves to position a taxon  
768 within the large groups of pterosaurs, but not among more taxonomically specific groups  
769 (Kellner, 2003; Unwin, 2003). In the case of SGO.PV.22805, it is not possible to calculate  
770 proportions between the tibiotarsus and the femur, since, although both elements are  
771 available, they are incomplete and were not found in association. Morphological characters  
772 of taxonomic significance have only been described in some derived pterosaurs as  
773 *Anhanguera piscator* (see Kellner and Tomida, 2000) and *Pteranodon* (see Bennett, 2001).  
774 Also, some features were described in some archaeopteroxyloids, for example  
775 *Wenupteryx uzi* (MOZ 3625P, see Codorniu and Gasparini, 2013), in which the tibia has a  
776 straight shaft, wider proximally than distally. Its diameter becomes smaller for one-quarter  
777 of the length, and then is constant up to the distal end. In *Wenupteryx*, the proximal tarsals  
778 seem fused to the tibia, but this region cannot be seen clearly and distal tarsals are damaged  
779 (Codorniu et al., 2006).

780 In addition, the tibiotarsus was described in "*Puntanipterus globosus*" (PVL 3869,  
781 see Bonaparte and Sanchez, 1975), whose synonymy with *Pterodaustro guinazui* was  
782 confirmed in Codorniu and Gasparini (2007). Tibia-fibulae of *Pterodaustro guinazui* in  
783 specimens with less postmortem compression (MIC-V169, MIC-V90) were compared to  
784 that of "*Puntanipterus*". The presence of a wide globose articulation, formed by the  
785 proximal tarsal bones (astragalus and calcaneum) fused to the tibia, as well as the presence  
786 of spiny processes on the medial and lateral sides of the distal end of the tibia were the most  
787 significant diagnostic features for these specimens. However, the presence of a spiny  
788 process in the lateral condyle of the tibia of PVL 3869 has not been observed in any other  
789 specimen. This feature was reported not as diagnostic of *Pterodaustro* but probably as an

790 ossified cartilage for the insertion of a tendon (lateral and medial ligamentous prominences  
791 described in Codorníu and Gasparini (2007). The great development of the wide globose  
792 articulation is also present in SGO.PV.22805, and it is similar to the tibiotarsus of  
793 *Pterodaustro* in that the lateral condyle extends proximomedially with a rounded proximal  
794 rim, while the medial condyle forms a rim with a medial concavity. The poor state of  
795 preservation of SGO.PV.22805 allows it to be referred to the Pterodactyloidea, probably an  
796 archaeopteroctyloid pterosaur.

797

## 798 **4. DISCUSIÓN**

### 799 **4.1. The pterosaurs of Cerro Tormento**

800 Although some of the bones show some degree of association with each other, most  
801 are completely disjointed. In addition, the presence of three humeri and one cervical  
802 vertebra from a small individual suggests that the materials preserved at Cerro Tormento  
803 belong to more than one individual. One of the main limitations when trying to classify the  
804 bones is that it cannot be assumed *a priori* that the entire set of bones belongs to the same  
805 taxon. This scenario is faced with the problem that most of the diagnosis of pterosaurs that  
806 allow taxonomic assignments is based on cranial material and dental characteristics  
807 (Wellnhofer, 1978). To a lesser extent, the diagnosis is based on cervical elements (Howse,  
808 1986), and to some extent based on the relative proportions of individual wing bones  
809 (Padian, 1991; Padian and Warheit, 1989; Padian and Wild, 1992).

810 The general morphology of the bones studied in this work suggests that they  
811 belonged to the clade Pterodactyloidea. Among these informative features are the large size  
812 of the bones, and the morphology of the glenoid of the scapulocoracoid, which is shared  
813 equally by both bones (Kellner, 2003; Unwin, 2003). Furthermore, the morphology of the

814 glenoid and the distal epiphysis of the humerus suggests that these bones belonged to  
815 pterosaurs that moved efficiently on the ground with their forelimbs under the body, which  
816 is a more widespread body posture among pterodactyloid pterosaurs (Fujiwara and  
817 Hutchinson, 2012; Witton, 2015). Additionally, there are some anatomical similarities  
818 between the bones described here and those belonging to some members of the  
819 Archaeopterodactyloidea, such as *Pterodaustro* (see comparisons in this paper).

820         The cervical vertebrae are the most informative elements found so far at Cerro  
821 Tormento, and correspond to post-axial elements of the mid cervical series. These vertebrae  
822 are procoelous, elongated, with a depressed neural arch and low neural spine (when  
823 preserved), features that are shared by the Ctenochasmatidae and Azhdarchidae. In the  
824 cervical vertebrae of azhdarchids, the neural arch is usually completely confluent with the  
825 vertebral centrum; this causes that the vertebra acquire a tubular-like morphology (Martill  
826 et al., 1998; Unwin, 2003; Andres and Ji, 2008; Witton and Naish, 2008). In contrast to  
827 azhdarchids, in the cervical vertebrae of ctenochasmatids, the depressed neural arch  
828 remains distinct from the vertebral centrum (Howse, 1986; Unwin, 2003; Andres and Ji,  
829 2008).

830         The cervical vertebrae from Cerro Tormento present a clear distinction between the  
831 neural arch and the vertebral centrum; the neural spine, when preserved, is low, rectangular,  
832 and anteroposteriorly elongated; so, these vertebrae are not tubular as in the  
833 Ctenochasmatidae. The presence of postexapophyses is a common feature in the  
834 Ornithocheiroidea (*sensu* Bennett, 1994; Kellner, 2003), and has been described in several  
835 azhdarchids (Andres and Ji, 2008; Andres et al., 2014; Lü et al., 2016). However, the  
836 postexapophyses are also present in some ctenochasmatids such as *Gegepterus changi*  
837 (Wang et al., 2007; Jiang and Wang, 2011) and *Elanodactylus prolatus* (Andres and Ji,

2008), although they seem to be absent in *Ctenochasma gracile* (Howse, 1986) and *Beipiaopterus chenianus* (Lü, 2003). In *Gegepterus changi*, the presence of cervical postexapophyses is one of the main features that suggest that this species is derived within the Archaeopterodactyloidea (Wang et al., 2007). Some authors have proposed that the independent acquisition of postexapophyses in the Ctenochasmatidae and Azhdarchidae is related to the strengthening and restriction of movement of the neck in large taxa, or those with a very long neck (Williston, 1897; Bennett, 2001; Andres and Ji, 2008). Another characteristic that suggests that the vertebrae from Cerro Tormento belong to the Ctenochasmatidae is the position of the neural canal. Martill et al., (2013) mentioned that in the Azhdarchidae the neural canal is centrally positioned with respect to the centrum, which according to these authors has not been reported so far in the Ctenochasmatidae. This feature seems to be more accentuated in anterior view, as can be observed in *Arambourgiania philadelphiae* (Martill et al., 1998) and *Azhdarcho lancicollis* (Nessov, 1984; Averianov, 2010). In the more complete mid cervical vertebra of Cerro Tormento, the neural canal in anterior view is very dorsally positioned as in the Ctenochasmatidae and contrary to that described in the Azhdarchidae by Martill et al. (2013). All these features mentioned are consistent with those described in the middle cervical vertebrae of pterosaurs of the Ctenochasmatidae (Kellner, 2003; Martill et al., 2013).

The evidence available so far suggests that the Cerro Tormento pterosaurs belong to the Archaeopterodactyloidea clade, and within this group, to the clade Ctenochasmatidae. These results confirm a second locality with ctenochasmatid pterosaurs in the Quebrada Monardes Formation. The middle cervical vertebrae found in Cerro Tormento are very similar in their morphology and size to that of two middle cervical vertebrae from Cerro La Isla, which were assigned to the Ctenochasmatidae by Alarcón-Muñoz et al. (2020). These

862 findings demonstrate that this group of pterosaurs were widespread in northern Chile during  
863 the Early Cretaceous.

864

#### 865 **4.2. Paleoenvironment and Paleobiology**

866         Among the stratigraphic section at Cerro Tormento, we recognized the presence of  
867 diagnostic sedimentary structures such as heterolithic cross-stratification which support the  
868 existence of an estuarine environment influenced by tides. Upon this evidence we suggest  
869 that a possible scenario for the genesis of the pterosaur preservation may have been  
870 deposition of sediments as result of water flows produced by tides in the proximities of a  
871 tidal channel. In contrast with Cerro Tormento, the southernmost pterosaur basin located at  
872 Cerro La Isla, indicates that pterosaur bones were preserved in high-energy water flows and  
873 sediments produced in a mainly continental environment. Compared to the stratigraphy  
874 documented in the locality of Cerro La Isla (Bell and Suarez, 1993; Bell and Padian, 1995),  
875 we could lithologically correlate the Cerro Tormento Section with the 250-350 m part of  
876 the section of Bell and Padian (1995; Fig. 4), which also include fine-grained facies and a  
877 pterosaur horizon and were interpreted as alluvial flood plains with ephemeral streams.  
878 Despite the similarities, the fine-grained facies association of Cerro Tormento (FA1) where  
879 interpreted as tidal plains, mainly because are overlaid and underlaid by cross bedded  
880 sandstones with inclined heterolithic stratification with mud draped foresets that were  
881 interpreted as tidal bars, and indicates proximity to the coast (Nio and Yang, 1991; Choi et  
882 al., 2004, Longhitano et al., 2012, Olariu et al., 2015; Tang et al., 2019). In Cerro La Isla,  
883 the alluvial flood plain levels are intercalated between large scale cross bedded sandstones  
884 interpreted as aeolian dune fields and there is major presence of channel lags,  
885 conglomerates and larger clast size which indicates alluvial systems in a flat desert plain ten

886 of kilometers inland from coast (Bell and Padian, 1995). Probably, the estuarine system of  
887 Cerro Tormento corresponds to river mouth and distal facies of the alluvial system of Cerro  
888 La Isla.

889 Preservation of pterosaur bones in marine or marine-influenced environments is  
890 relatively common. In fact, to date most of the currently known pterosaurs have been found  
891 in this type of environment (Butler et al. 2013, Upchurch et al. 2015). It is presumed this  
892 environment may have provided food to ctenochasmatid pterosaurs, probably consisting of  
893 crustaceans and other invertebrates (Qvarnström et al., 2019), also some small fishes.

894 Cerro Tormento would be one of the few cretaceous localities in the world in where  
895 several three-dimensional, well-preserved bones, belonging to more than one individual,  
896 have been preserved in the same constrained stratigraphic level. This new locality  
897 represents a valuable opportunity to carry out better and detailed stratigraphic studies  
898 comprising paleobiology and taphonomy of South American pterosaurs. Sequential  
899 stratigraphy studies in the Early Cretaceous of Quebrada Monardes Formation will be  
900 certainly important in order to recognize correlations between the known layer with  
901 pterosaur from Cerro Tormento and the previously recorded Cerro La Isla locality. Bell and  
902 Padian (1995) postulated the existence of one or more colonies of pterosaurs that lasted for  
903 a long time to explain the accumulation of pterosaur bones in Cerro La Isla, an idea that  
904 they support based on the existence of bones of immature individuals. The existence of a  
905 possibly similar context in Cerro Tormento, suggests the presence of an additional colony  
906 of pterosaurs, although, for now, there is no evidence of immature individuals. Additional  
907 taphonomical and sedimentological data are required for testing this hypothesis.

908 Although in Cerro La Isla and Cerro Tormento at least some pterosaurs belong to  
909 the Ctenochasmatidae, at the moment it is uncertain whether these pterosaurs belong to the

910 same species living along the extensive desert depression that existed in the area during the  
911 Lower Cretaceous. It is also not known whether the pterosaurs from both locations were  
912 approximately contemporaneous or belonged to one or more populations. For now, the  
913 middle cervical vertebrae are the only comparable element between the two locations. The  
914 middle cervical vertebrae of Cerro La Isla and Cerro Tormento have a similar size,  
915 morphology and proportions. These similarities suggest that the ctenochamatids from both  
916 localities probably belong to the same taxon. However, more comparable elements are  
917 needed to better support this idea.

918         The current evidence suggests that big colonies of ctenochasmatids inhabited in an  
919 extensive desert area, and at least, of those from Cerro Tormento, inhabited a coastal area  
920 during the Early Cretaceous. Both localities suggest that these ctenochasmatids had a  
921 gregarious behavior, although there is no certainty that this behavior has been maintained  
922 permanently or only temporarily as in reproductive season.

923         Gregarious behavior has been suggested for a few species of pterosaurs, such as the  
924 ctenochasmatid *Pterodaustro guinazui*, whose remains come from lacustrine sediments  
925 from the “Loma del *Pterodaustro*”, Lagarcito Formation (Lower Cretaceous), Argentina  
926 (Chiappe et al., 1998). The same has also been suggested for the tapejarid *Caiuajara*  
927 *dobruskii*, found in lacustrine deposits of the Goio-Erê Formation (Upper Cretaceous), of  
928 the Caiuá Group, Brazil (Manzig et al., 2014). The latter bears a special resemblance to the  
929 pterosaurs of the Quebrada Monardes Formation, since these tapejarids also lived in  
930 colonies in a desert environment. This indicates that this type of habitat was occupied by  
931 more than one type of gregarious pterosaur at different times in the group's history. Another  
932 possible evidence of social behavior is restricted to the finding of some specimens of  
933 *Quetzalcoatlus* in close proximity (Kellner, 1994). Additional examples includes duplicate



934 bones preserved in a concretion from the Romualdo Formation (Eck et al., 2011), two  
935 pterosaur specimens found in Kazakhstan (Costa et al., 2013), and an accumulation of eggs  
936 and bones from the pterosaur *Hamipterus tianshanensis* found in Lower Cretaceous rocks  
937 of China (Wang et al., 2017).

938         Considering the scarcity of sites in the world with accumulations of pterosaur  
939 bones, Cerro La Isla and Cerro Tormento have uncommon potential to provide evidence on  
940 social behavior in pterosaurs, which remains largely unknown in these animals.

941

## 942 5. CONCLUSIONS

943         A new locality with ctenochasmatid pterosaurs is described for the Lower  
944 Cretaceous in northern Chile. This deposit would have been formed in an estuarine  
945 environment, and bones would have been deposited under the influence of tides, and floods  
946 upon growth of river courses. Together with the “Cemitério dos pterossauros” in Brazil, the  
947 “Loma del *Pterodaustro*” in Argentina, the locality with *Hamipterus* in China, and Cerro  
948 La Isla in Chile, Cerros Bravos represents one of the few pterosaur localities in the world  
949 where associated remains belonging to several individuals have been found. The  
950 characteristics of this locality present an opportunity to carry out studies focused on aspects  
951 related to social behavior of these animals. On the other hand, the three-dimensional  
952 preservation of the bones allows the observation of characters that are not easily observed  
953 in other specimens, in which the bones are usually crushed, which often makes the analysis  
954 of osteological characters difficult.

955         The presence of the clade Ctenochasmatidae in Cerro Tormento and Cerro La Isla,  
956 separated from each other by more approximately 63 km, suggests that this clade, and  
957 potentially the same species, had an extensive distribution in what is now northern Chile,

958 although for now it cannot be assured that the pterosaurs from both sites were  
959 contemporary.

960 Most of the appendicular elements (i.e., tibiotarsus, humerus, pectoral girdle) alone,  
961 do not provide enough information to refer to them at a generic or specific level, but they  
962 can be referred to Pterodactyloidea, many of them having a special affinity to the clade  
963 Archaeopterodactyloidea. The vertebral remains described in this work were the most  
964 informative elements to elucidate more specific relationships of the pterosaurs of the  
965 Quebrada Monardes Formation with other known pterosaurs. These elements are referred to  
966 the clade Ctenochasmatidae, constituting new records of this group of pterosaurs.

967 Future prospection for Cerro Tormento and also Cerro La Isla will possibly allow  
968 obtaining more eloquent materials that will help elucidate whether the same species of  
969 ctenochasmatid is found at both sites. In addition, new stratigraphic studies accompanied by  
970 dating will make it possible to determine if both sites are synchronous. Finally, the  
971 discovery of a new pterosaur site in the Quebrada Monardes Formation suggests that more  
972 intensive prospecting in outcrops of this formation will possibly allow the discovery of new  
973 pterosaur species for Gondwana.

974

## 975 **Acknowledgement**

976 This research was supported by the Proyecto Anillo en Investigación en Ciencia y  
977 Tecnología (PIA, CONICYT) ACT172099 “New Data Sources on the Fossil Record and  
978 Evolution of Vertebrates”. National Council of Science of Argentina (CONICET);  
979 Universidad Nacional de San Luis, under grant CyT N°P-030520 to L.C.; Agencia  
980 Nacional de Promoción de la Investigación, el Desarrollo Tecnológico y la Innovación  
981 (AGENCIA), under the grant PICT-2017-0809 to L.C Logistics and field work were also

982 partially supported by Atacama Fossil Research. We thank Leslie Manríquez for her  
983 suggestions to the text. We also thank Roy Fernández Jiménez and Hermann Rivas for his  
984 support in the field. We thank S. Christopher Bennett and an anonymous reviewer for their  
985 valuable comments and suggestions, which helped improve the quality of this work.

986

## 987 REFERENCES

988 Aguirre-Urreta, M., 2001. Marine Upper Jurassic-Lower Cretaceous Stratigraphy  
989 and Biostratigraphy of the Aconcagua-Neuquén Basin, Argentina and Chile. *Journal of*  
990 *Iberian Geology* 27, 71–90.

991 Aguirre-Urreta, M., Mourgues, F., Rawson, P., Bulot, L., Jaillard, E., 2007. The  
992 Lower Cretaceous Chañarcillo and Neuquén Andean basins: ammonoid biostratigraphy and  
993 correlations. *Geological Journal* 42, 143–173.

994 Alarcón-Muñoz, J., Soto-Acuña, S., Rubilar-Rogers, D., González, E., Codorniú, L.,  
995 2018. Note on a new locality with pterosaurs (Archosauria: Pterodactyloidea) from the  
996 Atacama Region, Northern Chile. *Boletín del Museo Nacional de Historia Natural* 67(2),  
997 145–153.

998 Alarcón-Muñoz, J., Soto-Acuña, S., Codorniú, L., Rubilar-Rogers, D., Sallaberry,  
999 M., Suárez, M., 2020. New ctenochasmatid pterosaur record for Gondwana: discovery in  
1000 the Lower Cretaceous continental deposits of the Atacama Desert, northern Chile.  
1001 *Cretaceous Research* 110, 104378.

1002 Aleman, A., Ramos, V., 2000. The Northern Andes. In *Tectonic Evolution of South*  
1003 *America*, Cordani, U.G., Milani, E.J., Thomaz, Filho, A., Campos, D.A., (eds). 31st  
1004 *International Geological Congress: Río de Janeiro*, 453–480.

- 1005           Andres, B., Ji, Q., 2008. A new pterosaur from the Liaoning Province of China, the  
1006 phylogeny of the Pterodactyloidea, and convergence in their cervical vertebrae.  
1007 *Palaeontology*, 51 (2), 453–469.
- 1008           Andres, B., Clark, J.M., Xu. X., 2010. A new rhamphorhynchid pterosaur from the  
1009 Upper Jurassic of Xinjiang, China, and the phylogenetic relationships of basal pterosaurs.  
1010 *Journal of Vertebrate Paleontology* 30, 163–187.
- 1011           Andres, B., Clark, J., Xu, X., 2014. The earliest pterodactyloid and the origin of the  
1012 group. *Current Biology* 24, 1011–1016.
- 1013           Andres, B., Myers, T.S. 2013. Lone Star Pterosaurs. *Earth and Environmental*  
1014 *Science Transactions of the Royal Society of Edinburgh*, 103, 383–398.
- 1015           Andres, B., Langston, W., 2021. Morphology and taxonomy of *Quetzalcoatlus*  
1016 *Lawson 1975* (Pterodactyloidea: Azhdarchoidea). *Journal of Vertebrate Paleontology* 41(2),  
1017 46–202.
- 1018           Arambourg, C., 1954. Sur la presence d'un ptérosaurien gigantesque dans les  
1019 phosphates de Jordanie. *Comptes Rendus de L'Académie des Sciences Paris* 283, 133–134.
- 1020           Arévalo, C., 1995. Mapa Geológico de la hoja Copiapó, Región de Atacama.  
1021 Santiago. SERNAGEOMIN. Documentos de Trabajo n°008.
- 1022           Averianov, A.O., 2010. The osteology of *Azhdarcho lancicollis* Nesson, 1984  
1023 (Pterosauria, Azhdarchidae) from the Late Cretaceous of Uzbekistan. *Proceedings of the*  
1024 *Zoological Institute RAS*, 314 (3), 264–317.
- 1025           Bell, C.M., Suárez, M., 1989. Vertebrate fossil and trace fossils in Upper Jurassic  
1026 Lower Cretaceous red beds in the Atacama region, Chile. *Journal of South American Earth*  
1027 *Sciences*, 2 (4), 351–357.

- 1028 Bell, C.M., Padian, K., 1995. Pterosaurs fossils from the Cretaceous of Chile:  
1029 Evidence for a pterosaur colony on an inland desert plain. *Geological Magazine*, 132 (1),  
1030 31–38.
- 1031 Bennett, S.C., 1989. A Pteranodontid pterosaur from the early Cretaceous of Peru  
1032 with comments on the relationship of Cretaceous pterosaurs. *Journal of Paleontology* 63,  
1033 669–677.
- 1034 Bennett, S.C., 1991. Morphology of the late Cretaceous pterosaur *Pteranodon* and  
1035 the systematics of the Pterodactyloidea. Unpublished PhD dissertation, University of  
1036 Kansas, KS, 680 pp.
- 1037 Bennett, S.C., 1993. The ontogeny of *Pteranodon* and other pterosaurs.  
1038 *Paleobiology* 19, 92–106.
- 1039 Bennett, S.C., 1994. Taxonomy and systematics of the Late Cretaceous pterosaur  
1040 *Pteranodon* (Pterosauria: Pterodactyloidea). *Occasional Papers of the Natural History*  
1041 *Museum, University of Kansas*, 169, 1–70.
- 1042 Bennett, S.C., 2001. The osteology and functional morphology of the Late  
1043 Cretaceous pterosaur *Pteranodon*. I. General description of osteology. *Palaeontographica*,  
1044 *Abt. A*, 260, 1–112.
- 1045 Bennett, S.C., 2007. A review of the pterosaur *Ctenochasma*: taxonomy and  
1046 ontogeny. *Neues Jahrbuch für Geologie und Paläontologie-Abhandlungen* 245 (1), 23–31.
- 1047 Bennett, S.C. 2012. New information on body size and cranial display structures of  
1048 *Pterodactylus antiquus*, with revision of the genus. *Paläontologische Zeitschrift*, 87 (2),  
1049 269–289.
- 1050 Boggs Jr., S., 2009 *Petrology of Sedimentary Rocks*. 2nd Edition, Cambridge  
1051 University Press, New York, 600 p.

- 1052 Bonaparte, J.F. 1970. *Pterodaustro guiñazui*, pterosaurio de la Formación  
1053 Lagarcito, provincial de San Luis, Argentina, y su significado en la geología regional. Acta  
1054 Geológica Lilloana, 10; N° 10.
- 1055 Bonaparte, J.F., Sánchez, T.M., 1975. Restos de un pterosaurio *Puntanipterus*  
1056 *globosus* de la Formación La Cruz, Provincia de San Luis, Argentina. Actas Primer  
1057 Congreso Argentino de Paleontología y Bioestratigrafía, 2, 105–113.
- 1058 Buffetaut, E., Grigorescu, D., Csiki, Z., 2002. A new giant pterosaur with a robust  
1059 skull from the latest Cretaceous of Romania. Naturwissenschaften, 89, 180–184.
- 1060 Buffetaut, E., Laurent, Y., Le Leouff, J., Bilotte, M., 1997. A terminal Cretaceous  
1061 giant from the French Pyrenees. Geological Magazine, 134 (4), 553–556.
- 1062 Butler, R.J., Benson, R.B.J., Barrett, P.M., 2013. Pterosaur diversity: Untangling the  
1063 influence of sampling biases, Lagerstätten, and genuine biodiversity signals.  
1064 Palaeogeography, Palaeoclimatology, Palaeoecology 372, 78–87.
- 1065 Cai, Z., Wei, F., 1994. *Zhejiangopterus linhaiensis* (Pterosauria) from Upper  
1066 Cretaceous of Linhai, Zhejiang, China. Vertebrata Palasiatica, 32 (3), 181–194.
- 1067 Campos, D.A., Kellner, A.W.A. 1985. Panorama of the Flying Reptiles Study in  
1068 Brazil and South America. Anais da Academia brasileira de Ciências 57, 453–466.
- 1069 Casamiquela, R., 1975. *Herbstosaurus pigmaeus* (Coeluria; Compsognathidae)  
1070 n.gen. n.sp. del Jurásico medio de Neuquén (Patagonia septentrional). Uno de los más  
1071 pequeños dinosaurios conocidos. Actas Primer Congreso Argentino de Paleontología y  
1072 Bioestratigrafía. Tucumán 2, 87–102.
- 1073 Cerqueira, G.M., Santos, M.A.C., Marks, M.F., Sayão, J.M., Pinheiro, F.L., 2021. A  
1074 new azhdarchoid pterosaur from the Lower Cretaceous of Brazil and the  
1075 paleobiogeography of the Tapejaridae. Acta Paleontologica Polonica 66(3), 555–570.

- 1076           Chen, S., Steel, R.J., Dixon, J., Osman, A., 2014. Facies and architecture of a tide  
1077 dominated segment of the Late Pliocene Orinoco Delta (Morne L'Enfer Formation) SW  
1078 Trinidad. *Marine and Petroleum Geology* 57, 208–232.
- 1079           Chiappe, L.M., Rivarola, D., Romero, E., Dávila, S., Codorniú, L.S., 1998. Recent  
1080 advances in the paleontology of the lower Cretaceous Lagarcito Formation (Parque  
1081 Nacional Sierra de Las Quijadas, San Luis, Argentina). *New Mexico Museum of Natural  
1082 History and Science Bulletin*, 14, 187–192.
- 1083           Choi, K., Dalrymple, R., Chun, S., Kim, S., 2004. Sedimentology of Modern,  
1084 Inclined Heterolithic Stratification (IHS) in the Macrotidal Han River Delta, *Korea Journal  
1085 of Sedimentary Research* 74 (5), 677–689.
- 1086           Chotin, P., 1981. Dissymetrie fondamentale dans l'évolution des zones de  
1087 subduction de l'Ouest et de l'Est Pacifique depuis le Trias. *Société Géologique de France,  
1088 Bulletin*, (23), 245–252.
- 1089           Codorniú, L., Gasparini, Z. 2013. The Late Jurassic pterosaurs from northern  
1090 Patagonia, Argentina. *Earth and Environmental Science Transactions of the Royal Society  
1091 of Edinburgh* 103, 1–10.
- 1092           Codorniú, L., Gasparini, Z., Paulina-Carabajal, A., 2006. A late Jurassic pterosaur  
1093 (Reptilia, Pterodactyloidea) from northwestern Patagonia, Argentina. *Journal of South  
1094 American Earth Sciences*, 20, 383–389.
- 1095           Codorniú, L., Gasparini, Z., 2007. Pterosauria, 143–166. *In*: Gasparini, Z., Salgado,  
1096 L. y Coria, R. (Eds), *Patagonian Mesozoic Reptiles*. Indiana University Press, Bloomington  
1097 and Indianapolis, Indiana.
- 1098           Codorniú, L., Chiappe, L., Cid, F., 2013. First occurrence of stomach stones in  
1099 pterosaurs. *Journal of Vertebrate Paleontology*, 33(3), 647–654.

- 1100 Contreras, J., Jorquera, R., De La Cruz, R., Kraus, S., Ramírez, C., Naranjo, J.,  
1101 Espinoza, M., 2014. Carta Cerro del Pingo, Regiones de Antofagasta y de Atacama.  
1102 Santiago. SERNAGEOMIN. Carta Geológica de Chile, Serie Geología Básica n°169.
- 1103 Cornejo, P., Mpodozis, C., Tomlinson, A., 1998. Hoja Salar de Maricunga, Región  
1104 de Atacama (carta geológica 1:100.000). Servicio Nacional de Geología y Minería N° 7.  
1105 SERNAGEOMIN, Santiago, Chile.
- 1106 Cornejo P., Matthews, S., Mpodozis, C., Rivera, O., Riquelme, R., 2013. Carta El  
1107 Salvador, Región de Atacama. Santiago. SERNAGEOMIN. Carta Geológica de Chile,  
1108 Serie Geología Básica n°158.
- 1109 Costa, F.R., Alifanov, V., Dalla Vecchia, F.M., Kellner, A.W.A., 2013. On the  
1110 presence of an elongated tail in an undescribed specimen of *Batrachognathus volans*  
1111 Pterosauria: Anurognathidae: Batrachognathinae). In: Rio Ptero 2013-International  
1112 Symposium on Pterosaurs, Short Communications, 54–56.
- 1113 Creixell, C., Labbe, M., Arévalo, C., Salazar, E., 2013. Geología del área Estación  
1114 Chañar-Junta de Chingoles, regiones de Atacama y Coquimbo, Escala:1:100.000  
1115 [monografías]. Santiago: SERNAGEOMIN: 85 pp.
- 1116 Dong, Z., 1982. A new pterosaur (*Huanepterus quingyangensis* gen.et. sp.nov.)  
1117 from Ordos, China. *Vertebrata Palasiatica*, 20, 115–121 (In Chinese).
- 1118 Eaton, G.F., 1910. Osteology of *Pteranodon*. Connecticut Academy of Arts and  
1119 Sciences, memoirs, 2, 1–38.
- 1120 Eck, K., Elgin, R.A., Frey, E., 2011. On the osteology of *Tapejara wellnhoferi*  
1121 Kellner 1989 and the first occurrence of a multiple specimen assemblage from the Santana  
1122 Formation, Araripe Basin, NE-Brazil. *Swiss Journal of Palaeontology*, 130, 277–296.
- 1123 Erin, E.C., Arnott, R.W.C., 2007. Facies distribution and stratigraphic architecture



- 1124 of the Lower Cretaceous McMurray Formation, Lewis Property, northeastern Alberta. Bull.  
1125 Can. Pet. Geol., 55, 99–124.
- 1126 Fastnacht, M., 2005. The first dsungaripterid pterosaur from the Kimmeridgian of  
1127 the Germany and the biomechanics of pterosaur long bones. Acta Paleontológica Polonica  
1128 50 (2), 273–288.
- 1129 Fouquet, N., 2018. Registro fósil de secuencias marinas del Cretácico Inferior de la  
1130 Cuenca de Coloso, Norte de Chile (Unpubl. PhD thesis), Universidad Católica del Norte,  
1131 Universidad de Granada (2018), p. 323.
- 1132 Frey, E., Martill, D.M., 1996. A reappraisal of *Arambourgiania* (Pterosauria,  
1133 Pterodactyloidea): one on the world's largest flying animals. Neues Jahrbuch für Geologie  
1134 and Paläontologie, Abhandlungen, 199, 221–247.
- 1135 Fujiwara, S.I., Hutchinson, J.R., 2012. Elbow joint adductor moment arm as an  
1136 indicator of forelimb posture in extinct quadrupedal tetrapods. Proceedings of the Royal  
1137 Society B: Biological Sciences 279, 2561–2570.
- 1138 Godoy, E., Lara, L., 1998. Hojas Chañaral y Diego de Almagro, Región de  
1139 Atacama. Santiago. SERNAGEOMIN. Mapas Geológicos n°005-06.
- 1140 He, X., Yang, D., Su, C., 1983. A new Pterosaur from the Middle Jurassic of  
1141 Dashanpu, Zigong, Sichuan. Journal of the Chengdu College of Geology, Supplement 1,  
1142 27–33.
- 1143 Holz, M., 2003. Sequence stratigraphy of a lagoonal estuarine system-an example  
1144 from the lower Permian Rio Bonito Formation, Paraná Basin, Brazil. Sedimentary Geology,  
1145 162(3), 305–331.

- 1146 Hooley, R.W., 1913. On the skeleton of *Ornithodesmus latidens*; an ornithosaur  
1147 from the Wealden Shales of Atherfield (Isle of Wight). Quarterly Journal of the Geological  
1148 Society, London, 69, 372–421.
- 1149 Howse, S.C.B., 1986. On the cervical vertebrae of the Pterodactyloidea (Reptilia:  
1150 Archosauria). Zoological Journal of the Linnean Society, 88, 307–328.
- 1151 Iriarte, S., Arévalo, C., Mpodozis, C. 1999. Hoja La Guardia, Región de Atacama.  
1152 Servicio Nacional de Geología y Minería, Mapas Geológicos 3 (1:100.000). Santiago.
- 1153 Jablonski, B., Dalrymple, R., Marzo, M., 2016. Recognition of strong seasonality  
1154 and climatic cyclicality in an ancient, fluvially dominated, tidally influenced point bar:  
1155 Middle McMurray Formation, Lower Steepbank River, north-eastern Alberta, Canada.  
1156 Sedimentology (2016) 63, 552–585.
- 1157 Jiang, X., Wang, X., 2011. A new ctenochasmatid pterosaur from the Lower  
1158 Cretaceous western Liaoning, China. Anais da Academia Brasileira de Ciências, 83 (4),  
1159 1243–1249.
- 1160 Ji, S., Ji Q., 1997. Discovery of a new pterosaur in western Liaoning, China. Acta  
1161 Geologica Sinica, 71(2), 115–121.
- 1162 Kaup, J. J., 1834. Versuch einer eintheilung der saugethiere in 6 stämme und der  
1163 amphibian in 6 ordnungen. Isis 3, 311–315.
- 1164 Kellner, A.W.A., 1989. A new edentate pterosaur of the Lower Cretaceous from the  
1165 Ararape Basin, Northeast Brazil. Anais da Academia brasileira de Ciências 61, 439–446.
- 1166 Kellner, A.W.A., 1991. Supplementary comments to the Santana pterosaurs. In J.G.  
1167 Maisey (eds.), Santana Fossils, 370–371. Neptune City: T.F.H. Public.
- 1168 Kellner, A.W.A. 1994. Remarks on pterosaur taphonomy and paleoecology. Acta  
1169 Geologica Leopoldensia, 39, 175–189.

- 1170 Kellner, A.W.A., 1996. Description of new material of Tapejaridae and  
1171 Anhangueridae (Pterosauria, Pterodactyloidea) and discussion of pterosaur phylogeny. PhD  
1172 thesis, Columbia University. (Published by University Microfilms International), 347 pp.
- 1173 Kellner, A.W.A., 2003. Pterosaur phylogeny and comments on the evolutionary  
1174 history of the group. *In*: Buffetaut, E., Mazin, J.M. (eds.), *Evolution and Palaeobiology of*  
1175 *Pterosaurs*. Geological Society, London, Special Publication 217, 105–137.
- 1176 Kellner, A.W.A., 2013. A new unusual tapejarid (Pterosauria, Pterodactyloidea)  
1177 from the Early Cretaceous Romualdo Formation, Araripe Basin, Brazil. *Earth and*  
1178 *Environmental Science Transactions of the Royal Society of Edinburgh* 103, 1–13.
- 1179 Kellner, A.W.A., Tomida, Y., 2000. Description of a new species of Anhangueridae  
1180 (Pterodactyloidea) with comments on the pterosaur fauna from the Santana Formation  
1181 (Aptian-Albian), northeastern Brazil. *National Science Museum Monographs* N° 17, 147  
1182 pp.
- 1183 Kellner, A.W.A., Campos, D.A., Sayão, J.M., Saraiva, A.A.F., Rodrigues, T.,  
1184 Oliveira, G., Cruz, L.A., Costa, F.R., Silva, H.P., Ferreira, J.S., 2013. The largest flying  
1185 reptile from Gondwana: a new specimen of *Tropeognathus* cf. *T. mesembrinus* Wellnhofer,  
1186 1987 (Pterodactyloidea, Anhangueridae) and other large pterosaurs from the Romualdo  
1187 Formation, Lower Cretaceous, Brazil. *Anais da Academia Brasileira de Ciências* 85(1),  
1188 113–135.
- 1189 Kellner, A.W.A., Weinschütz, L.C., Holgado, B., Bantim, R.A.M., Sayão, J.M.,  
1190 2019. A new toothless pterosaur (Pterodactyloidea) from Southern Brazil with insights into  
1191 the paleoecology of a Cretaceous desert. *Anais da Academia Brasileira de Ciências* 91(2),  
1192 e20190768.
- 1193 Lara, L., Godoy, E., 1998. Hoja Quebrada Salitrosa, Región de Atacama.

- 1194 Santiago. SERNAGEOMIN. Mapas Geológicos nº004.
- 1195 Legarreta, L., Uliana, M. A. 1999. El Jurásico y Cretácico de la Cordillera Principal  
1196 y la Cuenca Neuquina. Facies Sedimentarias. In Geología Argentina, Caminos R (ed.).  
1197 Servicio Nacional Minero Geológico, Anales 29, 339–416.
- 1198 Li, S., Li, S., Shan, X., Gong, C., Yu, X., 2017. Classification, formation, and  
1199 transport mechanisms of mud clasts. *International Geology Review*, 59(12), 1609–1620.
- 1200 Longhitano, S.G., Donatella, M., Ronald, J.S., Ainsworth, R.B., 2012. Tidal  
1201 depositional systems in the rock record: A review and new insights. *Sediment. Geol.* 279,  
1202 2–22.
- 1203 Lü, J.C., 2003. A new pterosaur: *Beipiaopterus chenianus*, gen.et sp. nov. (Reptilia:  
1204 Pterosauria) from western Liaoning Province of China. *Memoir of the Fukui Prefectural*  
1205 *Dinosaur Museum* 2, 153–160.
- 1206 Lü, J., Gao, C., Meng, Q., Liu, J., Ji, Q., 2006. On the Systematic Position of  
1207 *Eosipterus yamgi* Ji et Ji, 1997 among Pterodactyloids. *Acta Geologica Sinica*, 80 (5), 643–  
1208 646.
- 1209 Lü, J., Kundrát, M., Shen, C., 2016. New Material of the Pterosaur  
1210 *Gladocephaloideus* Lü et al., 2012 from the Early Cretaceous of Liaoning Province, China,  
1211 with Comments on Its Systematic Position. *PLoS ONE* 11(6): E0154888. doi:  
1212 10.1371/journal.pone.0154888.
- 1213 Maahs, R., Kuchle, J., Scherer, C.M.S., Alvarenga, R.S., 2019. Sequence  
1214 stratigraphy of fluvial to shallow-marine deposits: The case of the early Permian Rio  
1215 Bonito Formation, Paraná Basin, southernmost Brazil. *Brazilian Journal of Geology*, 49(4),  
1216 1–21.

- 1217 Manzig, P.C., Kellner, A.W.A., Weinschutz, L.C., Fragoso, C.E., Vega, C.S.,  
1218 Guimaraes, G.B., Godoy, L.C., Liccardo, A., Ricetti, J.H.Z., De Moura, C.C., 2014. Desert  
1219 with insights on ontogeny and behavior of flying reptiles. PLoS ONE 9, 1–10.
- 1220 Martill, D.M., Frey, E., Sadaqah, R.M., Khoury, H.N., 1998. Discovery of the  
1221 holotype of the giant pterosaur *Titanopteryx philadelphiae* Arambourg 1959, and the status  
1222 of *Arambourgiania* and *Quetzalcoatlus*. Neues Jahrbuch für Geologie und Paläontologie -  
1223 Abhandlungen 207 (1), 57–76.
- 1224 Martill, D.M., Frey, E., Chong Diaz, G., Bell, C.M., 2000. Reinterpretation of a  
1225 Chilean pterosaur and the occurrence of Dsungaripteridae in South America. Geological  
1226 Magazine 137 (1), 19–25.
- 1227 Martill, D.M., Frey, E., Bell, C.M. Chong Diaz, G., 2006. Ctenochasmatid pterosaur  
1228 from Early Cretaceous deposits in Chile. Cretaceous Research 27, 603–610.
- 1229 Martill, D.M., O'Sullivan, M., Newman, C., 2013. A possible azhdarchid pterosaur  
1230 (Pterosauria, Azhdarchidae) in the Durlston Formation (Early Cretaceous, Berriasian) of  
1231 southern England. Cretaceous Research 30, 1–14.
- 1232 Matthews, S., Cornejo P., Riquelme, R., 2006. Carta Inca de Oro, Región de  
1233 Atacama. Santiago. SERNAGEOMIN. Carta Geológica de Chile, Serie Geología  
1234 Básica nº102.
- 1235 Mercado, M., 1982. Carta Geológica de Chile: Hoja Laguna del Negro Francisco,  
1236 Región de Atacama (includes map and memoir of 73 pp.). Servicio Nacional de Geología y  
1237 Minería, 56 (ISSN: 0716-0194).
- 1238 Miall, A.D., 1977. A review of the braided river depositional environment: Earth  
1239 Science Review, 13, 1–62.

- 1240 Miall, A.D.,1978. Lithofacies types and vertical profile models in braided river  
1241 deposits: A summary, *In*: Miall, A.D. (ed.), *Fluvial Sedimentology*: Canadian Society  
1242 Petrology Geology Memoir, 5, 597–604.
- 1243 Mourgues, A., 2004. Advances in ammonite biostratigraphy of the marine Atacama  
1244 basin (Lower Cretaceous), northern Chile, and its relationship with the Neuquén basin,  
1245 Argentina. *Journal of South American Earth Sciences* 17, 3–10.
- 1246 Mourgues, F. A., Bulot, L. G., Frau, C., 2015. The Valanginian *Olcostephaninae*  
1247 Haug, 1910 (Ammonoidea) from the Andean Lower Cretaceous Chañarcillo Basin,  
1248 Northern Chile. *Andean Geology*, 42(2), 213–236.
- 1249 Mpodozis, C., Allmendinger, R. 1993, Extensional tectonics, Cretaceous Andes,  
1250 northern Chile (27°S): *Geological Society of America Bulletin*, 105, 1462–1477.
- 1251 Mpodozis, C., Iriarte, S., Gardeweg, M., Valenzuela, M. 2012. Carta Laguna del  
1252 Negro Francisco, Región de Atacama. Santiago. SERNAGEOMIN. Carta Geológica de  
1253 Chile, Serie Geología Básica n°145.
- 1254 Mpodozis, C., Clavero, J., Quiroga, R., Droguett, B., Arcos, R., 2018. Geología del  
1255 área de Cerro Cadillal-Cerro Jotabeche, Región de Atacama.  
1256 Santiago. SERNAGEOMIN. Carta Geológica de Chile, Serie Geología Básica n°200.
- 1257 Musial, G., Reynaud, J.Y., Gingras, M., Fenies, H., Labourdette, R., Parize, O.,  
1258 2012. Subsurface and outcrop characterization of large tidally influenced point bars of the  
1259 Cretaceous McMurray Formation (Alberta, Canada). *Sediment. Geol.* 2012, 11, 156–172.
- 1260 Muzzio, G., 1980. Geología de la region comprendida entre el Cordón el Varillar y  
1261 Sierra de Viscachas, Precordillera de Atacama. Unpublished Thesis, Universidad de Chile.
- 1262 Nessonov, L.A., 1984. Upper Cretaceous pterosaurs and birds from central Asia.  
1263 *Paleontologicheskii Zhurnal*, 1984 (1), 47–57 (In Russian).

- 1264 Nio, S.-D., Yang, C.-S., 1991. Diagnostic attributes of clastic tidal deposits: a  
1265 review. In: Smith, D.G., Reinson, G.E., Zaitlin, B.A., Rahmani, R.A. (Eds.), *Clastic Tidal*  
1266 *Sedimentology*: Canadian Society of Petroleum Geologists. Memoir, 16, 3–28.
- 1267 Nopcsa, F., 1928. The genera of reptiles. *Palaeobiologica*, 1, 163–188.
- 1268 Olariu, M.I., Olariu, C., Steek, R.J., Dalrymple, R.W., Martinius, A.W., 2012.  
1269 Anatomy of a laterally migrating tidal bar in front of a delta system: Esdolomada Member,  
1270 Roda Formation, Tremp-Graus Basin, Spain. *Sedimentology* 59, 356–378.
- 1271 Olariu, C., Steel, R.J., Olariu, M.I., Choic, K.S., 2015. Facies and architecture of  
1272 unusual fluvialtidal channels with inclined heterolithic strata: Campanian Neslen  
1273 Formation, Utah, USA. In: Ashworth, P.J., Best, J.L., Parsons, D.R. (eds.), *Fluvial- Tidal*  
1274 *Sedimentology*. Elsevier, Amsterdam, The Netherlands, 353–394.
- 1275 Padian, K., 1983. Osteology and functional morphology of *Dimorphodon macronyx*  
1276 (Buckland) (Pterosauria: Ramphorynchoidea) based on new material in the Yale Peabody  
1277 Museum. *Postilla* 189, 1–44.
- 1278 Padian, K., 1991. Pterosaurs; were they functional birds or functional bats? In:  
1279 *Biomechanics and Evolution* (eds. J. M. V. Rayner y R. J. Wootton), 145–160. Cambridge  
1280 University Press.
- 1281 Padian, K., 2008. The Early Jurassic pterosaur *Dorygnathus banthensis* (Theodori,  
1282 1830). *Special Papers in Paleontology* 80, 1–64.
- 1283 Padian, K., Warheit, K.I., 1989. Morphometrics of pterosaur wing: one sharp  
1284 division, few trends. *Journal of Vertebrate Paleontology* 9 (suppl. 3), 35 A. Padian, K.,  
1285 Wild, R. 1992. Studies of Liassic Pterosauria. I. The holotype and referred specimens of the  
1286 Liassic pterosaur *Dorygnathus banthensis* (Theodori) in the Petrefaktensammlung Banz,  
1287 northern Bavaria. *Palaeontographica, Abteilung A*, 225, 59–77, 5 pls.

- 1288 Pemberton, S.G., Flach, P.D., Mossop, G.D., 1982. Trace fossils from the Athabasca  
1289 oil sands, Alberta, Canada. *Science* 1982, 217, 825–827.
- 1290 Plieninger, F. 1894. "*Campylognathus zitteli*", ein neuer Flugsaurier aus dem  
1291 obersten Lias Schwabens", *Paläontographica* 41, 193–222 and pl. 19.
- 1292 Plieninger, F. 1901. Beiträge zur Kenntnis der Flugsaurier. *Palaeontographica* 48,  
1293 65–90.
- 1294 Plieninger, F., 1907. Die Pterosaurier der Juraformation Schwabens.  
1295 *Paleontographica*, 53, 209–313. Stuttgart.
- 1296 Plint A.G. 2010. Wave- and storm-dominated shoreline and shallow-marine  
1297 systems. In: James N.P., Dalrymple R. W. (Eds.), *Facies models 4 Newfoundland &*  
1298 *Labrador*, Geological Association of Canada Publications, 4, 167–199.
- 1299 Qvarnström, M., Elgh, E., Owocki, K., Ahlberg, P.E., Niedźwiedzki, G., 2019.  
1300 Filter feeding in Late Jurassic pterosaurs supported by coprolite contents. *PeerJ* 7: e7375  
1301 <http://doi.org/10.7717/peerj.7375>
- 1302 Ramos, V.A., 2009. Anatomy and Global Context of the Andes: Main Geologic  
1303 Features and the Andean Orogenic Cycle. *In: The Geological Society of America, Memoir*,  
1304 204 pp.
- 1305 Ramos, V., Naipauer, M., Leanza, H., Sigismondi, M. 2019. The Vaca Muerta  
1306 Formation of the Neuquén Basin: An Exceptional Setting along the Andean Continental  
1307 Margin, *In: Daniel Minisini, Manuel Fantin, Iván Lanusse, and Héctor Leanza, (eds.),*  
1308 *Integrated geology of unconventional: The case of the Vaca Muerta play, Argentina:*  
1309 *AAPG Memoir* 120, DOI: 10.1306/13682222M1202855.
- 1310 Rauhut, O.W.M., López-Arbarello, A., Röper, M., Rothgaenger, M., 2017.  
1311 Vertebrate fossils from the Kimmeridgian of Brunn: the oldest fauna from the Solnhofen



- 1312 Archipelago (Late Jurassic, Bavaria, Germany). *Zitteliana* 89, 305–329.
- 1313 Reineck, H.E., Wunderlich, F., 1968. Classification and origin of flaser and  
1314 lenticular bedding. *Sedimentology* 11, 99–104.
- 1315 Rodrigues, T., Kellner, A.W.A., Mader, B.J., Russell, D.A., 2011. New pterosaur  
1316 specimens from the Kem Kem beds (Upper Cretaceous, Cenomanian) of Morocco. *Rivista*  
1317 *Italiana di Paleontologia e Stratigrafia*, 117 (1), 149–160.
- 1318 Romer, A.S. 1956. *Osteology of the Reptiles*. Chicago: University of Chicago  
1319 Press: xxi + 772 pp.
- 1320 Tang, M., Zhang, K., Huang, J., Lu, S. 2019. Facies and the Architecture of  
1321 Estuarine Tidal Bar in the Lower Cretaceous McMurray Formation, Central Athabasca Oil  
1322 Sands, Alberta, Canada. *Energies* 2019, 12, 1769.
- 1323 Theodori, C., 1852. Ueber die *Pterodactylus* Knochen im Lias von Banz. *Berichte*  
1324 *des naturforschenden Vereins zu Bamberg* 1, 17–44.
- 1325 Tucker, M.E., 2003. *Sedimentary Rocks in the Field*. Department of Geological  
1326 Sciences, University of Durham, Durham, 252.
- 1327 Tucker, M.E., 2011. *Sedimentary Rocks in the Field: A Practical Guide*. 4th  
1328 Edition, John Willey and Sons Ltd., Chichester, 85–104.
- 1329 Unwin, D.M., 2003. On the phylogeny and evolutionary history of pterosaurs, In:  
1330 Buffetaut, E., Mazin, J.-M. (Eds.), *Evolution and Palaeobiology of Pterosaurs*. Geological  
1331 Society, London, Special Publication 217, 139–190.
- 1332 Unwin, D.M., 2006. *The pterosaurs from the deep time*. Nèraumont Publishing  
1333 Company, New York, 347 pp.
- 1334 Unwin, D. M., Lü, J., Bakhurina, N.N., 2000. On the systematic and stratigraphic  
1335 significance of pterosaurs from the Lower Cretaceous Yixian Formation (Jehol Group) of

- 1336 Liaoning, China. *Mitteilungen aus dem Museum für Naturkunde, Berlin,*  
1337 *Geowissenschaftlich, Reihe, 3, 181–206.*
- 1338 Upchurch, P., Andres, B., Butler, R.J., Barret, P.M., 2015 An analysis of  
1339 pterosaurian biogeography: implications for the evolutionary history and fossil record  
1340 quality of the first flying vertebrates. *Historical Biology, 27(6), 697–717.*
- 1341 Venegas, C., Cervetto, M., Astudillo, N., Espinosa, F., Cornejo, P., Mpodozis, C.,  
1342 Rivera, O., 2013. *Carta Sierra Vaquillas Altas, Región de Antofagasta. Servicio Nacional*  
1343 *de Geología y Minería, Carta Geológica de Chile, Serie Geología Básica N° 159, 1, mapa*  
1344 *escala 1: 100.000. 87 pp. Santiago.*
- 1345 Wang, X., Kellner, A.W.A., Jiang, S., Cheng, X., Wang, Q., Ma, Y., Paidoula, Y.,  
1346 Rodrigues, T., Chen, H., Sayão, J.M., Li, N., Zhang, J., Bantim, R.A.M., Meng, X., Zhang,  
1347 X.; Qiu, R. y Zhou, Z. 2017. Egg accumulation with 3D embryos provides insight into the  
1348 life history of a pterosaur. *Science 385, 1197–1201.*
- 1349 Wang, X., Kellner, A.W.A., Zhou, Z., De Almeida Campos, D., 2007. A new  
1350 pterosaur (Ctenochasmatidae, Archaeopterodactyloidea) from the Lower Cretaceous Yixian  
1351 Formation of China. *Cretaceous Research 28, 245–260.*
- 1352 Wellnhofer, P., 1970. *Die Pterodactyloidea (Pterosauria) der Oberjura-Platenkalke*  
1353 *Süddeutschlands. -Abhandlung der Bayerischen Akademie der Wissenschaften, Neue*  
1354 *Folge, 141, 1–133.*
- 1355 Wellnhofer, P. 1975., *Die Rhamphorhynchoidea (Pterosauria) der Oberjura-*  
1356 *Plattenkalke Süddeutschlands. Teil 1: Allgemeine Skelettmorphologie. Palaeontographica*  
1357 *A 148, 1–33.*
- 1358 Wellnhofer, P. 1978., *Pterosauria. Handbuch der Paläoherpetologie, Teil 19.*  
1359 *Stuttgart. New York: Gustav Fischer Verlag. 82 pp.*

- 1360 Wellnhofer, P., 1991. The illustrated Encyclopedia of Pterosaurs. Salamander  
1361 Books, London. 192 pp.
- 1362 Williston, S.W., 1903. On the osteology of *Nyctosaurus* (*Nyctodactylus*), with notes  
1363 on American pterosaurs. Field Columbian Museum Publication, Geological Series, 2, 125–  
1364 163.
- 1365 Williston, S.W., 1897. Restoration of *Ornithostoma* (*Pteranodon*). Kansas  
1366 University Quartely, Series A, 6, 35–51.
- 1367 Witton, M. P. 2013. Pterosaurs: Natural History, Evolution, Anatomy. Princeton  
1368 University Press, 304 pp.
- 1369 Witton, M.P., 2015. Were early pterosaurs inept terrestrial locomotors? PeerJ 3, 1–  
1370 32, e1018; DOI 10.7717/peerj.1018.
- 1371 Witton, M.P., Naish, D., 2008. A reappraisal of azhdarchid pterosaur functional  
1372 morphology and paleoecology. PLoS ONE, 3, e2271. doi: 10.1371/journal.pone.0002271.
- 1373 Witton, M.P., 2007. Titans of the skies: azhdarchid pterosaurs. Geology Today 23,  
1374 33–38.
- 1375 Young, C., 1964. On a new pterosaurian from Sinkiang, China. Vertebrata  
1376 PalAsiatica 8, 221–255.

1377

## 1378 **FIGURE CAPTIONS**

1379 **Figure 1.** A) The southwestern margin of Gondwana with the locations of Lower  
1380 Cretaceous basins, modified from Aguirre-Urreta et al. (2007) B) Lower Cretaceous  
1381 geological units of Chañarcillo Basin and Pterosaur bones localities: Cerro Tormento and  
1382 Cerro La Isla. The geological units' polygons are based in (Arévalo, 1995; Cornejo et al.,  
1383 1998; Godoy and Lara, 1998; Lara and Godoy, 1998; Matthews et al., 2006; Mpodozis et

1384 al., 2012; Cornejo et al., 2013; Contreras et al., 2014; Mpodozis et al., 2018).

1385

1386 **Figure 2.** Stratigraphic section of Quebrada Monardes in Cerro Tormento locality.

1387

1388 **Figure 3.** Sedimentary facies in Cerro Tormento Section: (A) F1, laminated purple reddish  
1389 mudstones and fine-grained sandstones; (B) Rippled cross lamination, flaser bedding and  
1390 mud drapes in F2; (C) Rippled cross lamination and locally bioturbated sandstones in F2  
1391 *Pl: Planolites* isp.; (D) F3a, planar stratified coarse sandstone beds with rounded pebbles;  
1392 (E) F3b mud clast breccia; and (F) Bi-directional crossbeds (herringbone cross  
1393 stratification) in the lee-side area of a compound dune.

1394

1395 **Figure 4.** (A) Site of pterosaur bones recollection; (B) Pterosaur bones at Facies 3b at the  
1396 top of the section; (C) Inclined heterolithic lamination, note the thin mud drapes on the  
1397 foresets and the ripples with mud drapes at the base of cross beds; (D) Asymmetrical linguoid  
1398 ripples in Facies 2 near the top of section.

1399

1400 **Figure 5.** Ctenochasmatidae indet., SGO.PV.22800, vertebra of the middle cervical series  
1401 (left) and schematic representations (right), in anterior (A), posterior (B), left lateral (C),  
1402 dorsal (D), right lateral (E) and ventral (F) views. Abbreviations: na: neural arch; nc: neural  
1403 canal; con: condyle; cot: cotyle; dep: depression; hyp: hypapophysis; poex:  
1404 postexapophysis; poz: postzygapophysis; prex: preexapophysis; prz: prezygapophysis; vc:  
1405 vertebral centrum; vls: ventro-lateral sulcus. Scale: 20 mm.

1406

1407 **Figure 6.** Ctenochasmatidae indet., SGO.PV.22801, vertebra of the middle cervical series

1408 in dorsal view (A) and its cast (B) together with their respective diagrams. SGO.PV.22804.  
1409 C) Incomplete mid-series cervical vertebra in ventral view and schematic interpretation.  
1410 SGO.PV.22815, incomplete cervical vertebra of the middle series in dorsolateral view (D)  
1411 and interpretive scheme. Abbreviations: ns: neural spine; prz: prezygapophysis; vc:  
1412 vertebral centrum Scale: 10 mm. Abbreviations: na: neural arch; nc: neural canal; con:  
1413 condyle; cot: cotyle; dep: depression; hyp: hypapophysis; poex: postexapophysis; poz:  
1414 postzygapophysis; prex: preexapophysis; prz: prezygapophysis; vc: vertebral centrum; vls:  
1415 ventro-lateral sulcus. Scale: 20 mm.

1416

1417 **Figure 7.** Archaeopterodactyloidea indet., SGO.PV.22805, impression of a right  
1418 scapulocoracoid (A) and schematic representation in lateral view from a silicone mold  
1419 obtained from it. SGO.PV.22810, left coracoid in dorsal (C), posterior (D), anterior (E), and  
1420 ventral (F) views and schematic interpretations. Abbreviations: asfs: articular surface for  
1421 sternum; cgc: coracoidal glenoid cavity; dep: depression; cor: coracoid; sc: scapula; gf:  
1422 glenoid fossa; cp: coracoid process; prcorp: procoracoid process.; sgp: supraglenoid  
1423 process; tub: tubercle. Scale bar: 10 mm.

1424

1425 **Figure 8.** Archaeopterodactyloidea indet., SGO.PV.22806, impression of the incomplete  
1426 humerus and a fragment of an indeterminate appendicular element (A) and schematic  
1427 interpretation. SGO.PV.22807, incomplete left humerus together with indeterminate  
1428 elements (B) and schematic interpretation. Abbreviations: dpc: deltopectoral crest; dia:  
1429 diaphysis; ect: ectepicondyle; ent: entepicondyle; ie: indeterminate element; de: distal  
1430 epiphysis; hum: humerus. Scale bar: 10 mm. Scale bars: 10 mm.

1431

1432 **Figure 9.** Archaeopterodactyloidea indet., SGO.PV.22808, distal portion of the right  
1433 humerus and their respective interpretative diagrams in posterior (A), distal (B) and anterior  
1434 (C) views. Abbreviations: cap: capitulum; dia: diaphysis; ect: ectepicondyle; ent:  
1435 entepicondyle; ig: intercondylar groove; tro: trochlea. Scale bar: 10 mm.

1436

1437 **Figure 10.** Archaeopterodactyloidea indet., SGO.PV.22814. Impression of an incomplete  
1438 left femur and schematic representation from a silicone counter mold. Abbreviations: fh:  
1439 femoral head; fn: femoral neck; dia: diaphysis; et: external trochanter. Scale bar: 10 mm.

1440

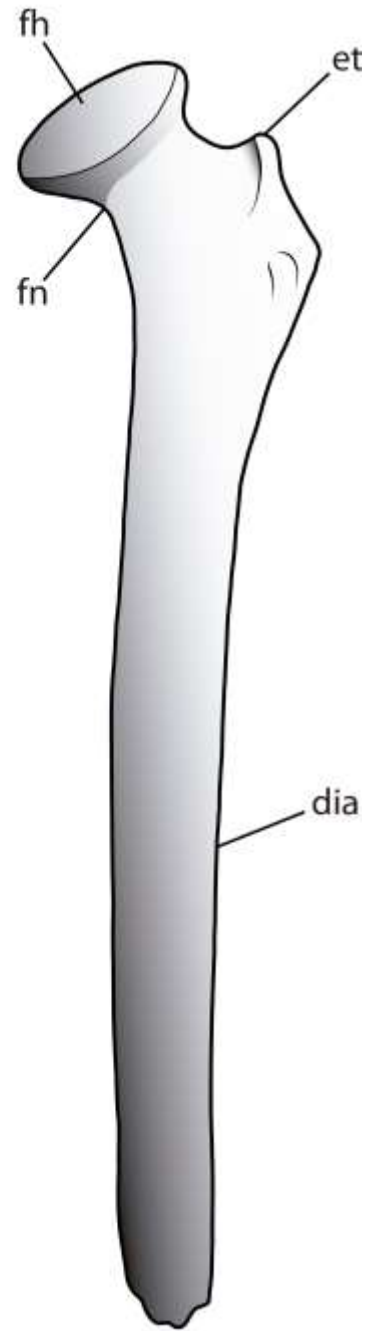
1441 **Figure 11.** Pterodactyloidea indet., SGO.PV.22805. Incomplete impression of the anterior  
1442 surface of a left tibiotarsus and scheme made from a silicone mold obtained from the  
1443 impression. Abbreviations: lac: lateral condyle; mec: medial condyle; di: diaphysis; ig:  
1444 intercondylar groove. Scale bar: 10 mm.

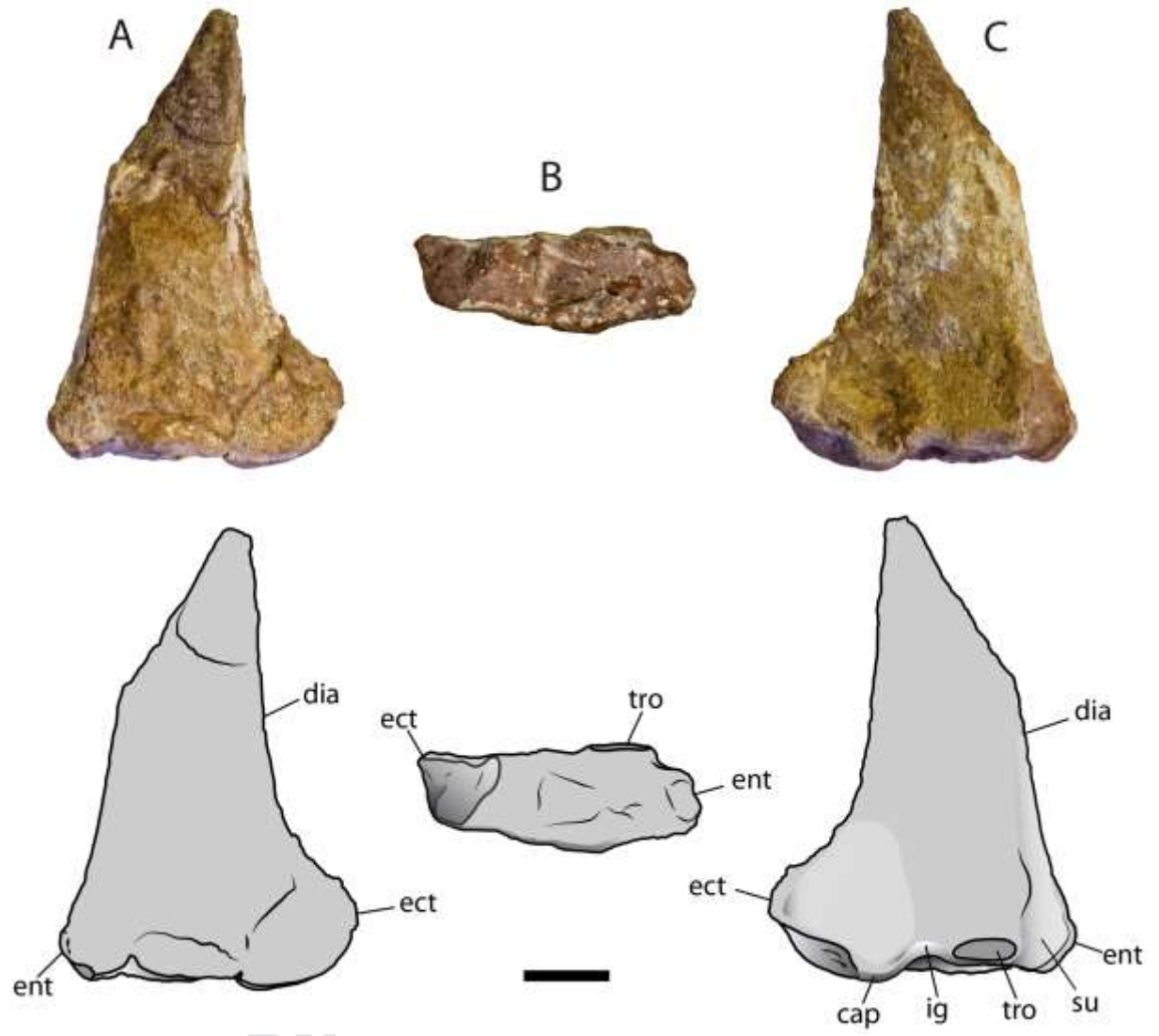
1445

1446

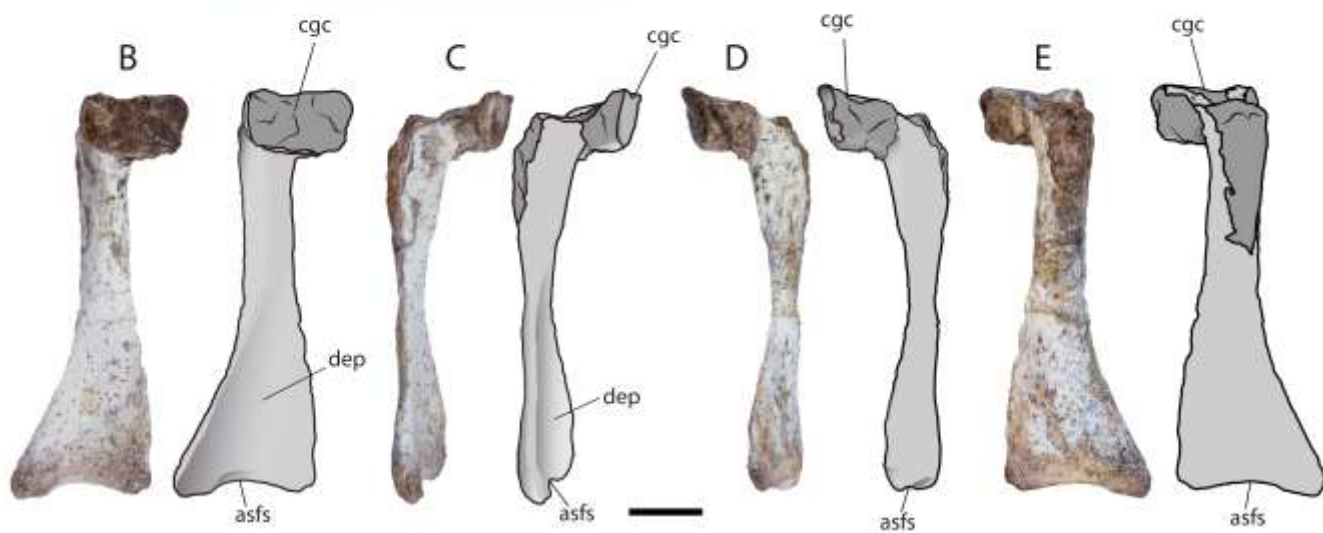
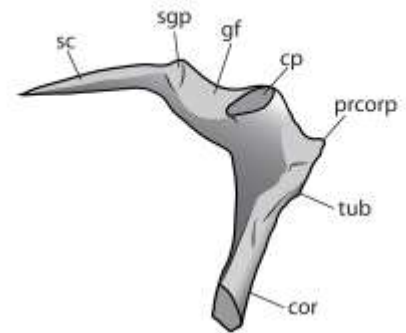
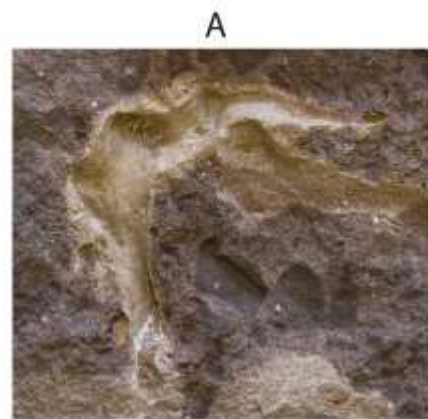
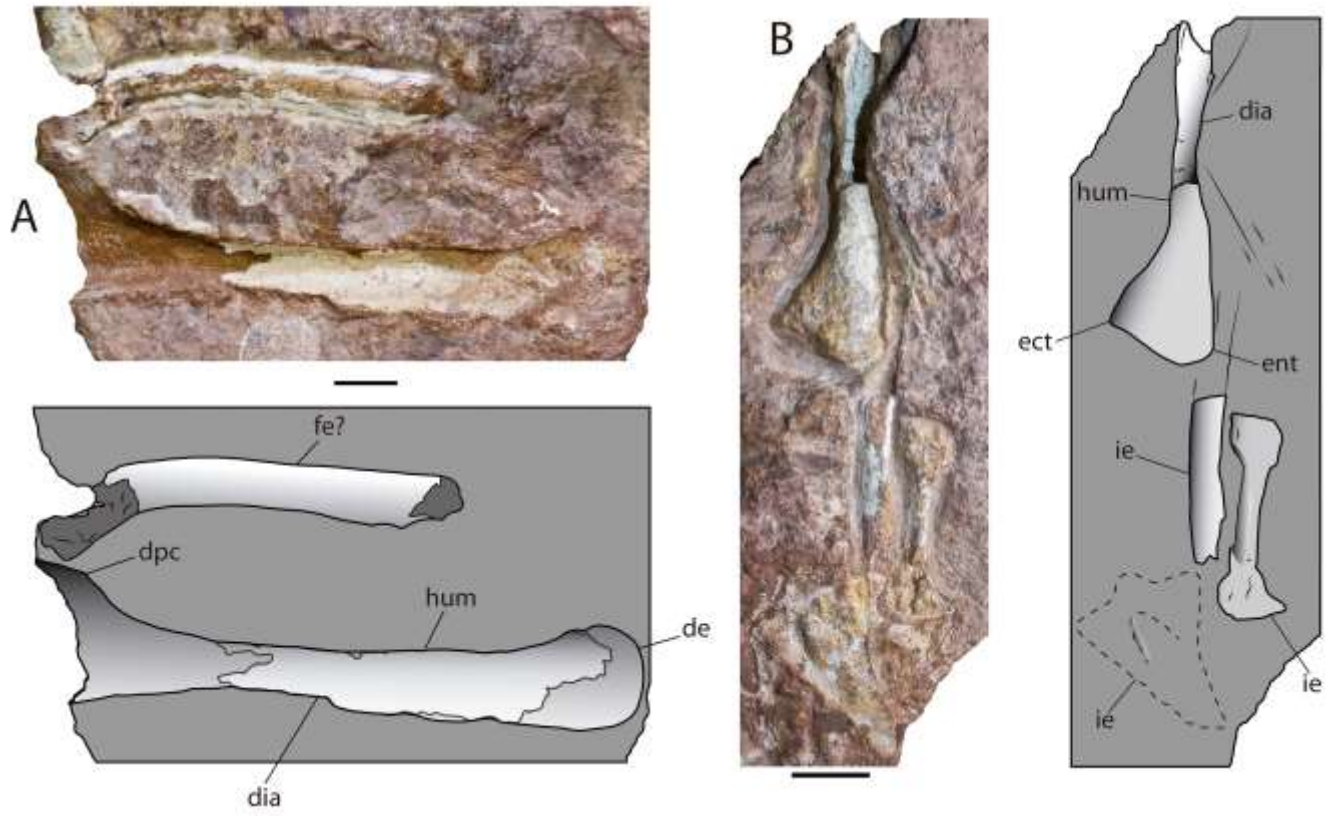
1447

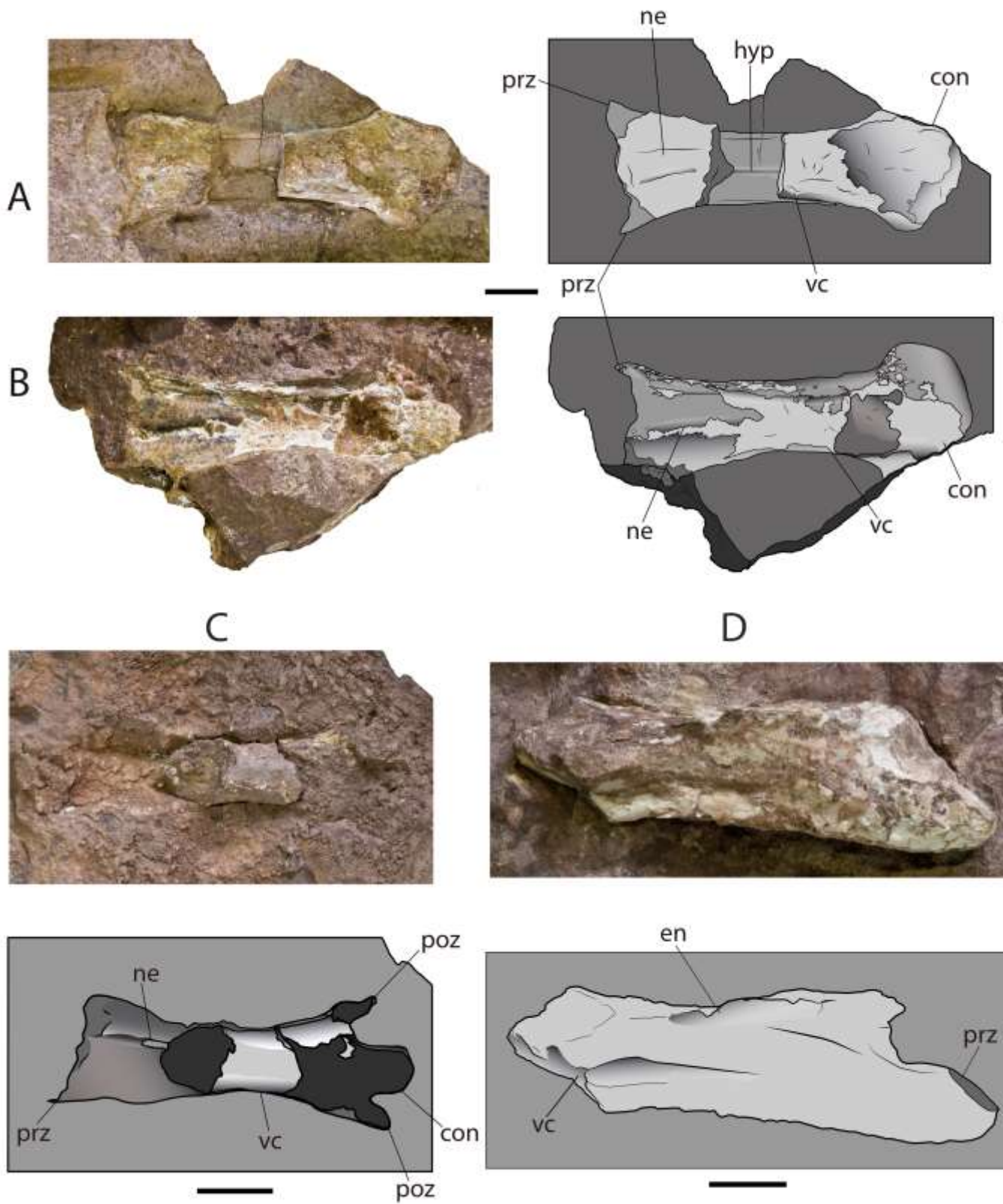
1448

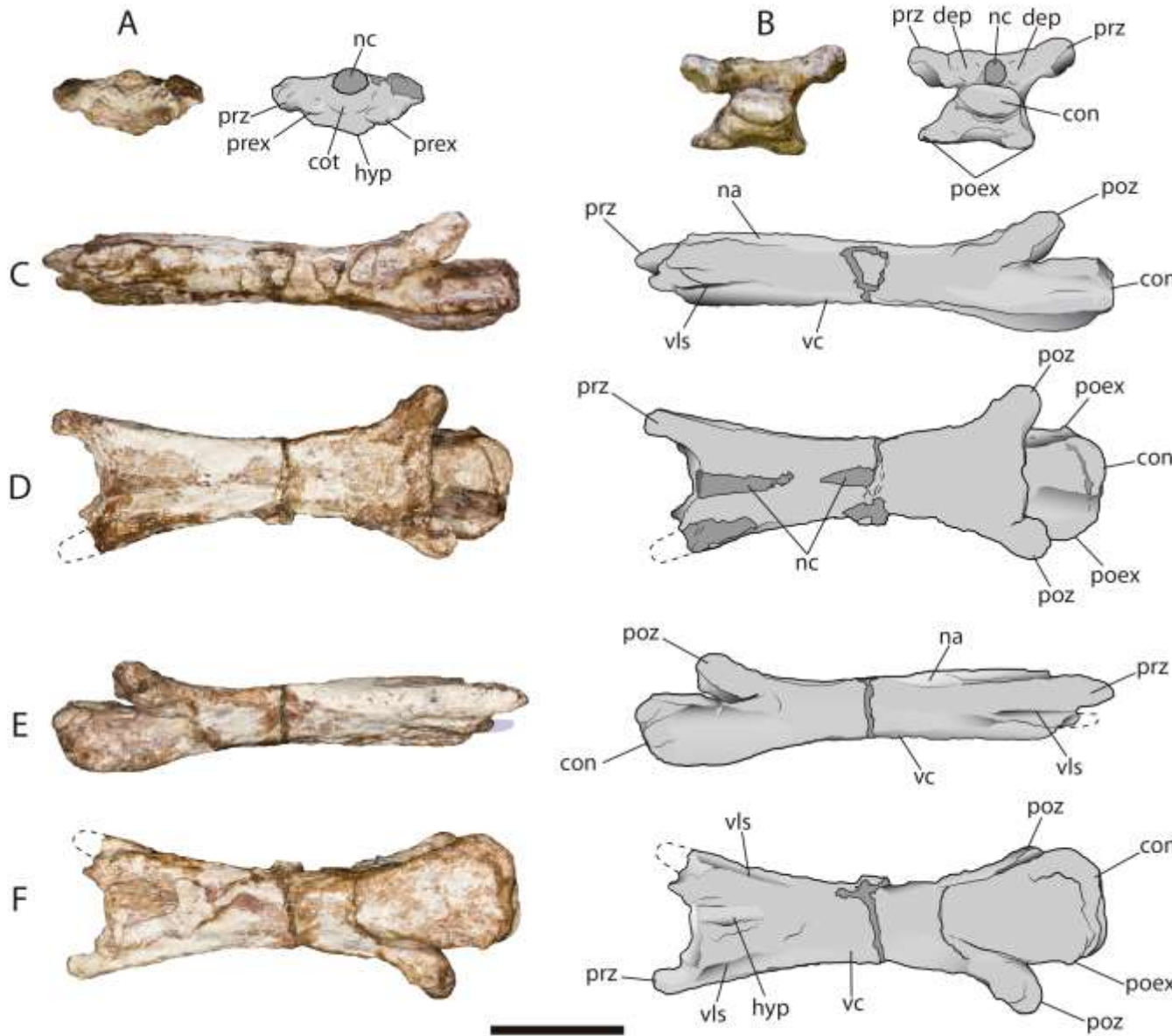


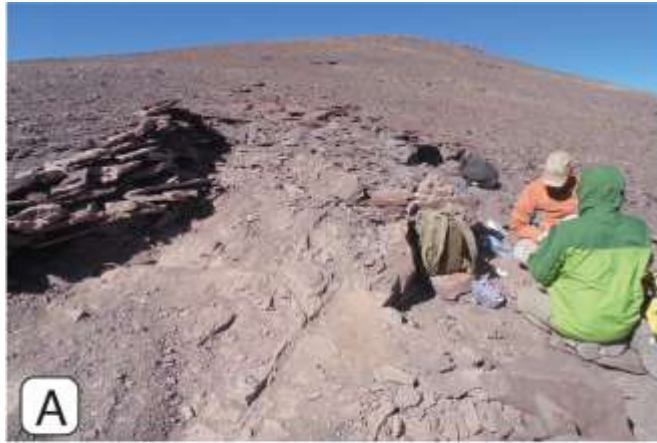




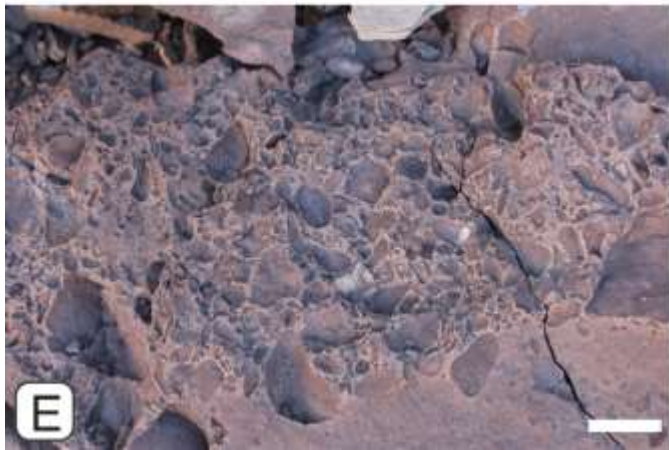
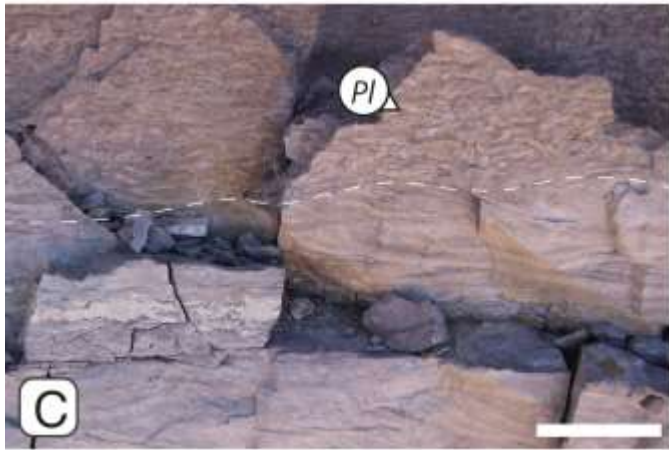




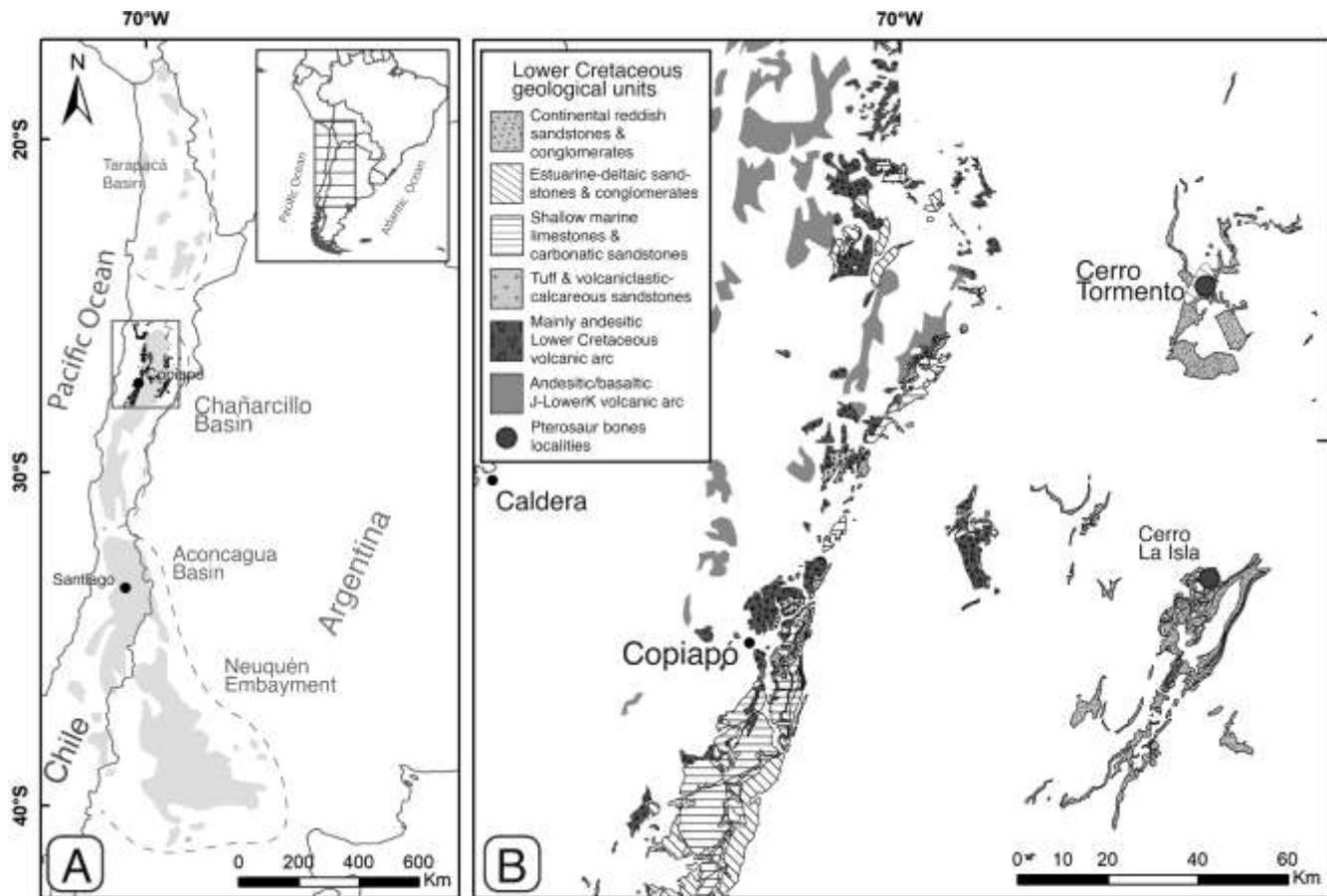


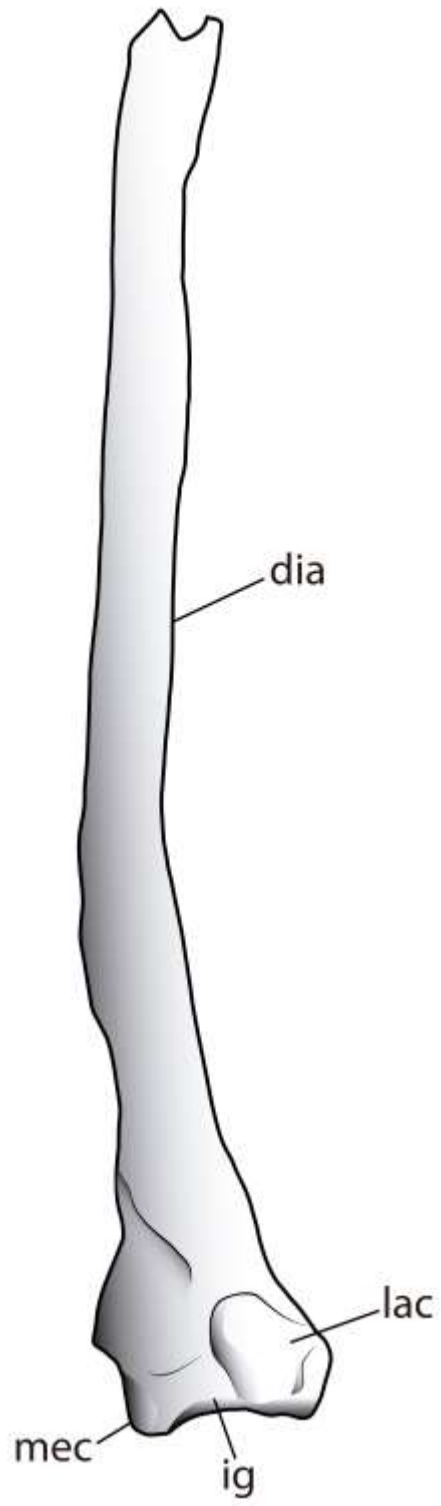


Journal











### **Highlights**

- 1.** A second Lower Cretaceous locality with pterosaurs is reported in the Atacama Desert, northern Chile.
- 2.** Cerro Tormento represents a new locality with ctenochamatid pterosaurs in the Atacama Desert.
- 3.** This discovery shows that the clade Ctenochasmatidae had a wide geographic distribution in what is now northern Chile during the Lower Cretaceous.

### Sample Credit Author Statement

**Manuscript:** A new locality with ctenochasmatid pterosaurs (Pterosauria: Pterodactyloidea) in the Atacama Desert, Northern Chile

**Jhonatan Alarcón-Muñoz**, investigation, methodology, conceptualization, formal analysis, visualization, writing - review & editing; **Laura Codorniú**, investigation, conceptualization, formal analysis, supervision, validation, writing - review & editing; **Edwin González**, investigation, visualization, writing - review & editing; **Mario E. Suárez**, investigation, resources, writing - review & editing; **Manuel Suárez**, investigation, validation, writing - review & editing; **Omar Vicencio-Campos**, writing - review & editing; **Sergio Soto-Acuña**, investigation, validation, writing - review & editing; **Jonatan Kaluza**, writing - review & editing; **Alexander O. Vargas**, resources, validation, writing - review & editing, Founding acquisition; **David Rubilar-Rogers**, validation, writing - review & editing, resources.

**Declaration of interests**

The authors declare that they have no known competing financial interests or personal relationships that could have appeared to influence the work reported in this paper.

The authors declare the following financial interests/personal relationships which may be considered as potential competing interests:

Journal Pre-proof